

RESEARCH ARTICLE

The mevalonate pathway is a crucial regulator of tendon cell specification

Jessica W. Chen^{1,2,*}, Xubo Niu^{1,*}, Matthew J. King¹, Marie-Therese Noedl¹, Clifford J. Tabin² and Jenna L. Galloway^{1,‡}

ABSTRACT

Tendons and ligaments are crucial components of the musculoskeletal system, yet the pathways specifying these fates remain poorly defined. Through a screen of known bioactive chemicals in zebrafish, we identified a new pathway regulating tendon cell induction. We established that statin, through inhibition of the mevalonate pathway, causes an expansion of the tendon progenitor population. Co-expression and live imaging studies indicate that the expansion does not involve an increase in cell proliferation, but rather results from re-specification of cells from the neural crest-derived *sox9a⁺/sox10⁺* skeletal lineage. The effect on tendon cell expansion is specific to the geranylgeranylation branch of the mevalonate pathway and is mediated by inhibition of Rac activity. This work establishes a novel role for the mevalonate pathway and Rac activity in regulating specification of the tendon lineage.

KEY WORDS: Tendon, Scleraxis, Chemical screen, Statin, Zebrafish

INTRODUCTION

Tendons and ligaments are key components of the musculoskeletal system, transmitting and stabilizing high tensile forces. Exposed to such forces, adult tendons are often injured during overuse, trauma or age-related decline (Jozsa and Kannus, 1997). Knowledge of tendon fate determination has important implications for developing regenerative approaches to treating tendon injuries. Although the basic helix-loop-helix transcription factor scleraxis (*Scx*) provides a marker of early tendon and ligament progenitors (Schweitzer et al., 2001), the pathways leading to tendon cell fate induction remain largely unknown.

Scx marks tendon and ligament cells in all anatomical locations (Brent et al., 2003; Grenier et al., 2009; Schweitzer et al., 2001), and is required for the development of the limb force-transmitting tendons (Murchison et al., 2007). *Scx* also regulates the expression of extracellular matrix proteins – including *Colla1* – through its proximal promoter (Léjard et al., 2007). The identification of *Scx* as a marker of early tendon progenitors opened the door to studies of factors involved in tendon specification. TGF β signals are sufficient to induce *Scx* expression in mesenchymal tissues (Havis et al., 2014; Pryce et al., 2009). However, mouse genetic loss-of-function

studies indicate a role for this pathway in tendon cell maintenance, rather than induction (Oka et al., 2008; Pryce et al., 2009; Tan et al., 2020). An important role for FGF signaling was identified in the specification of axial tendon progenitors in the chick (Brent et al., 2003; Brent and Tabin, 2004), yet the tendon-promoting effect of FGF signaling is not conserved in mouse, as highlighted in studies showing that early FGF/ERK signaling represses *Scx* expression in mouse (Havis et al., 2014, 2016).

Although the crucial pathways responsible for tendon cell specification remain unknown, studies examining neighboring tissues provide insights into the interactions required for their specification. In the craniofacial, axial and limb regions, tendon and ligament cells form in close association with skeletal cells and are thought to arise from common progenitors (Soeda et al., 2010). The cranial skeletal and tendon progenitors are derived from the cranial neural crest (CNC) (Chen and Galloway, 2014; Couly et al., 1993; Kontges and Lumsden, 1996; Le Douarin and Kalcheim, 1999; Le Lievre, 1978; Lumsden et al., 1991; Noden, 1978; Schilling and Kimmel, 1994); in the limb, they are derived from the lateral plate mesoderm (Hurle et al., 1989, 1990; Kieny and Chevallier, 1979; Pearse et al., 2007; Ros et al., 1995; Saunders, 1948; Wortham, 1948); and in axial regions, tendon progenitors, which form the syndetome, are derived from the early sclerotome, a somitic compartment (Brand-Saberi and Christ, 2000; Brent et al., 2003; Monsoro-Burq and Le Douarin, 2000). *Sox9* is expressed in chondrogenic cells, and common *Sox9/Scx* co-expression domains are found at tendon-bone attachment sites (Blitz et al., 2013; Sugimoto et al., 2013). Furthermore, loss of transcription factors important for cartilage differentiation results in ectopic expression of tendon markers within the axial rib cartilage structures (Brent et al., 2005). Although this effect was not observed in cranial or limb regions, mammalian *in vitro* studies suggest that tendon and cartilage are mutually exclusive lineages of common progenitor populations (Havis et al., 2014).


To discover new pathways that govern tendon cell induction, we turned to the zebrafish, a system that is highly amenable to high-throughput small molecule screening (Mathias et al., 2012). Previous zebrafish chemical screens have expanded our understanding of developmental processes and identified compounds of potential therapeutic benefit (Goessling and North, 2014; North et al., 2007), highlighting the conservation between zebrafish and humans. Zebrafish tendons share many similarities with those in mammals, including gene expression, morphology, collagen ultrastructural arrangement and developmental regulation (Chen and Galloway, 2014; Subramanian and Schilling, 2014). We therefore reasoned that chemical screens of biologically annotated bioactives in zebrafish could reveal new pathways regulating tendon development.

In a small-molecule whole-embryo screen, we identified statins as regulators of early tendon specification. Statins are a class of 3-hydroxy-3-methylglutaryl-coenzyme A reductase (HMGCR)

¹Center for Regenerative Medicine, Harvard Stem Cell Institute, Department of Orthopedic Surgery, Massachusetts General Hospital, Harvard Medical School, 185 Cambridge Street, Boston, MA 02114, USA. ²Department of Genetics, Harvard Medical School, 77 Avenue Louis Pasteur, Boston, MA 02115, USA.

*These authors contributed equally to this work

‡Author for correspondence (jenna_galloway@hms.harvard.edu)

 J.W.C., 0000-0003-4425-6369; J.L.G., 0000-0003-3792-3290

inhibitors that are prescribed as cholesterol-lowering agents (Istvan and Deisenhofer, 2001). In addition to preventing cardiovascular disease, statins and HMGCR pathway inhibition regulate cell proliferation in tumors (Jones et al., 1994) and cell migration during heart and germ cell development (D'Amico et al., 2007; Santos and Lehmann, 2004; Thorpe et al., 2004; Yi et al., 2006). Using chemical and genetic approaches, we show that Hmgcr inhibition expands the number of craniofacial and pectoral fin tendon progenitors in the zebrafish embryo. The expansion is not a consequence of increased proliferation of a pre-existing *scleraxis*-positive (*scxa*⁺) cell population, but rather is caused by recruitment of additional neural crest *sox9a*⁺/*sox10*⁺ skeletal progenitors towards tendon fates. We further demonstrate through loss-of-function studies that the interaction is mediated by inhibition of the geranylgeranylation branch of the mevalonate pathway, and specifically Rac GTPases. Taken together, we establish that the mevalonate pathway via Rac activity is a crucial regulator of tendon fate specification.

RESULTS

Statin promotes tendon cell expansion in zebrafish craniofacial and pectoral fin regions

To identify new pathways regulating tendon development in zebrafish, we conducted a chemical screen using a known bioactive compound library: NINDS Custom Collection 2. Wild-type embryos were incubated with individual chemicals from 32 to 56 h post-fertilization (hpf) and examined at 56 hpf by whole-mount *in situ* hybridization for altered craniofacial expression of *scxa* (a *scx* paralogue in zebrafish) (Fig. 1A). These stages were chosen to identify pathways affecting tendon cell induction, as *scxa* is first detected in the zebrafish pharyngeal arches by 40 hpf (Chen and Galloway, 2014) (Fig. S1). Our screen identified lovastatin and simvastatin (Fig. S2A–D) as agents that increase craniofacial *scxa* expression. Additional statins, atorvastatin and fluvastatin, similarly expand craniofacial *scxa* expression (Fig. S2E–L). All statin compounds used in this study inhibit HMGCR and have some differences in their metabolism and pharmacokinetic properties (Klotz, 2003). Atorvastatin caused the most robust phenotype in the cranial and fin regions (Fig. 1B,C,F,G), and most analysis was performed with this compound. Atorvastatin treatment from 48 to 72 hpf resulted in a similar *scxa* expansion at 72 hpf when assessed by whole-mount *in situ* hybridization (Fig. 1D,E,H,I). Analysis of fluvastatin, which has the shortest half-life among statins (Igel et al., 2001), demonstrated the 32–48 hpf treatment window was sufficient to expand craniofacial *scxa* expression (Fig. S2M–R). The statin-mediated upregulation of *scxa* was further confirmed by qPCR at both stages (Fig. 1J). Quantification of *scxa*⁺ cells using whole-mount *in situ* hybridization or Tg(*scxa:mcherry*) zebrafish (Fig. S3I–Q) verified that statin treatment increases the number of *scxa*⁺ cells in the craniofacial (Fig. 1L) and pectoral fin (Fig. 1M, Fig. S3B) regions compared with controls. At the stages examined, the Tg(*scxa:mcherry*) line was found to recapitulate endogenous *scxa* expression (Fig. S1). Although early (32–56 hpf) and later (48–72 hpf) treatments resulted in expanded *scxa* expression, it is possible that the cellular mechanism underlying expansion is not identical between the stages. Because the early treatment was better tolerated by embryos and resulted in less toxicity, we focused on dissecting the effects of statin treatment in the 32–56 hpf stages.

To test whether statin expands expression of additional tendon genes, as opposed to simply upregulating *scxa* expression, we examined expression of *colla2*, which is expressed during tendon differentiation and is a major component of the tendon extracellular matrix (Brent et al., 2003; Chen and Galloway, 2014). We found that

embryos incubated with atorvastatin also have expanded *colla2* expression (Fig. S2W–X). Likewise, statin causes >2-fold increase in the number of craniofacial *colla2*⁺ tendon progenitors compared with controls (Fig. 1N) and increases *colla2* expression by qPCR (Fig. 1K). As forming bone is rich in type I collagen, we examined expression of *runx2a*, a marker of osteoblasts (Burns et al., 2002), following statin treatment. We found that *runx2a* expression was not qualitatively expanded at 56 hpf and was decreased at 72 hpf (Fig. S2S–V), suggesting that the increase in *colla2* expression is due to expanded tendon fates. Besides the head and fin, *scxa*⁺ tendon progenitors in zebrafish exist in the myosepta, connecting the muscles of the trunk. In contrast to the pectoral fin and craniofacial region, atorvastatin does not affect the quantity of *scxa*⁺ (Fig. S2Y) or *scxa:mcherry*⁺ (Fig. S2Y–C') cells in the myosepta. Furthermore, atorvastatin treatment from 32–56 hpf reduced myoseptal *colla2* expression at 74 hpf (Fig. S2D'–E'). Although the differences in response to statin treatment in the different anatomical locations may be derived from tissue-specific differences in drug efficaciousness, we hypothesize the difference is more reflective of region-specific programs of tendon development (Brent et al., 2003; Chen and Galloway, 2014).

Statin-mediated expansion of tendon progenitors does not depend on increased proliferation

In principle, the increased quantity of tendon progenitors could arise from increased proliferation of *scxa*⁺ cells. To determine whether statin increases tendon cell proliferation, we performed EdU labeling (Salic and Mitchison, 2008) and phospho-histone H3 (PH3) staining. EdU pulse-labeling at 4 or 5 h intervals of chemically treated embryos transgenic for a neural crest and cranial cartilage reporter, *sox10:mcherry* (Fig. 2A–B'), indicated that atorvastatin does not increase the number of proliferative cells in anatomically defined regions compared with corresponding regions in controls (Fig. 2C). Rather, we observed a trend of decreased proliferation following atorvastatin treatment at 43 hpf, 52 hpf and 56 hpf, suggesting that the mevalonate pathway regulates proliferation in the craniofacial region. The mevalonate pathway negatively affects proliferation in other cell types (Corsini et al., 1993; Gong et al., 2019). Given that subtle changes in proliferation within the *scxa*⁺ domain may not be detected with this analysis, we performed two sets of experiments to address this concern. First, we quantified the number of PH3⁺ mitotic cells in atorvastatin-treated and control embryos. Consistent with our EdU findings, we determined that atorvastatin does not promote proliferation in the craniofacial or fin regions (Fig. S3A,C). More importantly, we did not detect any increase in the ratio of PH3⁺/*scxa*⁺ cells in either region (Fig. 2D,E,H and Fig. S3D,I,L–Q). Second, we hypothesized that if the statin-mediated expansion were acting through increased cell proliferation, an antimetabolic agent would abrogate its effect. We analyzed the effect of aphidicolin, a DNA polymerase inhibitor (Spadari et al., 1984), on proliferation and craniofacial *scxa* expression with and without statin treatment. The concentration of aphidicolin used reduces the quantity of PH3⁺ cells (Fig. 2D,F and Fig. S3A) (Ladstein et al., 2010) as well as the total number of *scxa*⁺ cells in DMSO-treated embryos (Figs 1L, 2D,F,I and Fig. S3E,F). This indicates that proliferation contributes to the expansion of *scxa*⁺ cells during normal development in control DMSO-treated embryos. Strikingly, atorvastatin and aphidicolin co-treatment from 32 to 56 hpf caused >2-fold expansion in craniofacial *scxa*⁺ cells (Fig. 2E,G,I and Fig. S3G,H), compared with aphidicolin treatment alone, indicating that inhibiting proliferation has no effect on the ability of statin to expand tendon cell number.

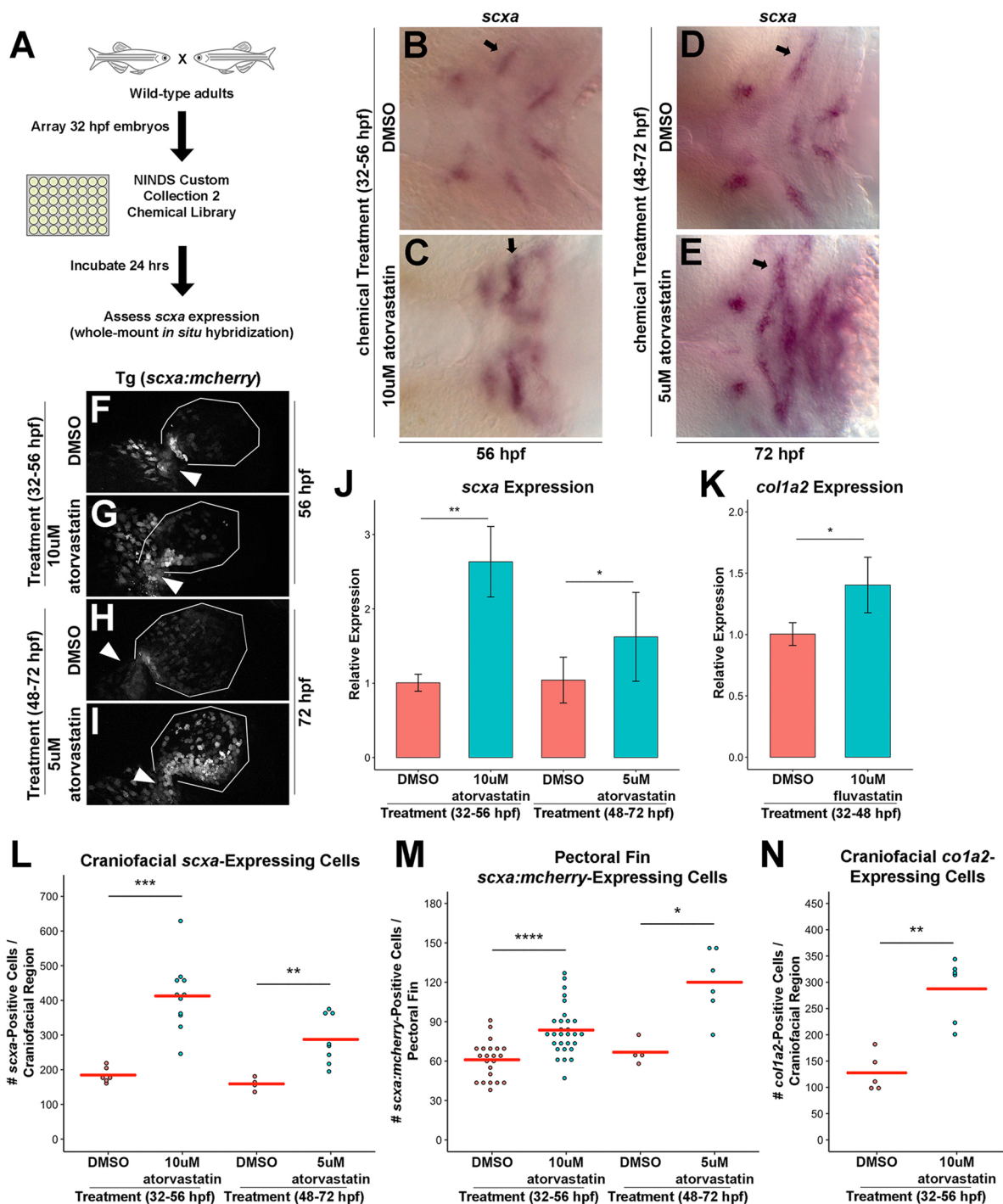


Fig. 1. A zebrafish chemical screen identifies statins as regulators of craniofacial and pectoral fin tendon progenitors. (A) Design of the small-molecule screen. Wild-type embryos were incubated with individual compounds from 32 to 56 hpf and alterations in craniofacial *scxa* expression were assessed at 56 hpf. (B-E) Craniofacial *scxa* expression at 56 hpf, after incubation from 32 to 56 hpf (B,C) and at 72 hpf after incubation from 48 to 72 hpf (D,E). Atorvastatin expanded *scxa* expression in the pharyngeal arches (arrows) compared with controls. (F-I) Pectoral fin *scxa:mcherry* expression at 56 hpf (F,G) and 72 hpf (H,I) upon incubation from 32 to 56 hpf and 48 to 72 hpf, respectively. Atorvastatin expanded *scxa:mcherry* expression at the cleithrum base (arrowhead), extending distally to the actinotrichia. (J) qPCR quantification revealed that atorvastatin increased *scxa* expression at 56 hpf and 72 hpf upon incubation from 32 to 56 hpf and 48 to 72 hpf, respectively, compared with controls. $n=4$, whole embryo (32-56 hpf) and head region (48-72 hpf); Welch's two-tailed *t*-test. (K) qPCR quantification revealed that fluvastatin increased *col1a2* expression at 72 hpf, after incubation from 32 to 48 hpf compared with controls. The combination of fluvastatin, which is characterized by a shorter half-life and a shortened exposure window (Fig. S2M-R), mitigated the toxic effects observed at 72 hpf with atorvastatin treatment. $n=3$, head region, Welch's two-tailed *t*-test. (L) Atorvastatin increased the quantity of craniofacial *scxa*⁺ cells at 56 hpf and 72 hpf after incubation from 32 to 56 hpf and 48 to 72 hpf, respectively, compared with controls. (M) Atorvastatin increased the quantity of pectoral fin *scxa:mcherry*⁺ cells at 56 hpf and 72 hpf upon incubation from 32 to 56 hpf and 48 to 72 hpf, respectively, compared with controls. (N) Atorvastatin increased the quantity of *col1a2*⁺ cells at 80 hpf, after incubation from 32 to 56 hpf compared with controls. (J,K) Data are mean \pm s.d. (L-N) Red bars indicate mean; individual points represent values for individual embryos; Mann-Whitney-Wilcoxon test. * $P<0.05$; ** $P<0.01$; *** $P<0.001$; **** $P<0.0001$. Ventral (B-E) and lateral (F-I) views, anterior towards the left.

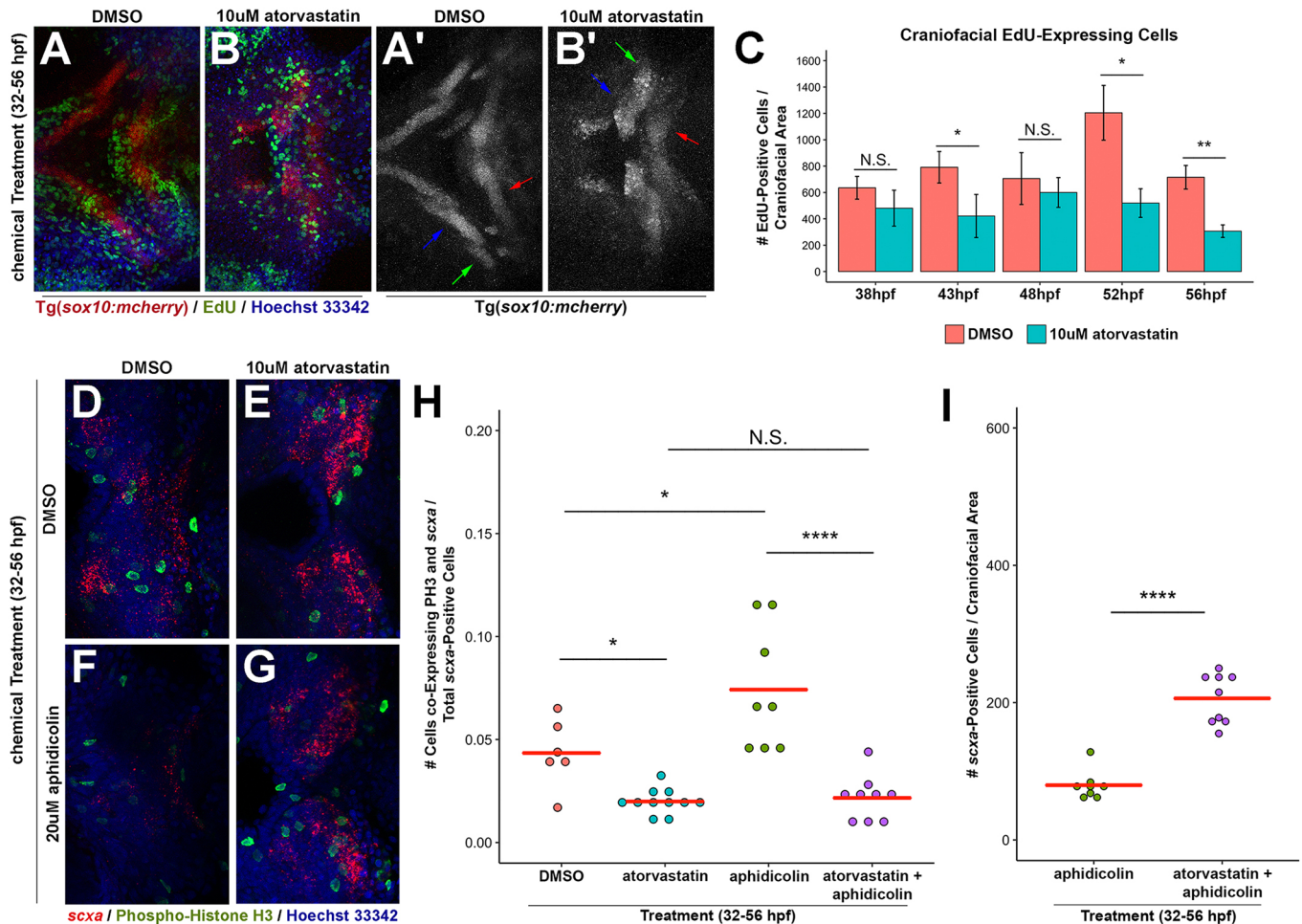


Fig. 2. Statin-mediated expansion of craniofacial tendon progenitors is not due to increased proliferation of *scxa*-positive cells. (A,B) *Tg(sox10:mcherry)* embryos at 56 hpf were chemically treated from 32 to 56 hpf, labeled for EdU⁺ cells and counterstained with Hoechst. Arrows in A',B' mark Meckel's cartilage (blue), palatoquadrate cartilage (green) and ceratohyal cartilage (red). (C) Quantification of EdU⁺ cells in the craniofacial region upon incubation from 32 hpf. Atorvastatin does not increase the quantity of craniofacial EdU⁺ cells at timepoints examined, compared with controls. $n=3$, Welch's two-tailed *t*-test. Data are mean \pm s.d. (D-G) Craniofacial expression of *scxa* and phospho-histone H3 (PH3) at 56 hpf upon incubation with the indicated compounds from 32 to 56 hpf. Craniofacial *scxa* expression compared with controls (D) is reduced in aphidicolin-treated embryos (F), and expanded in embryos treated with atorvastatin alone (E) and in combination with aphidicolin (G). Data from these representative images are plotted in H,I and Fig. S3A. (H) Quantification of craniofacial cells co-expressing PH3 and *scxa* at 56 hpf after incubation from 32 to 56 hpf. (I) Quantification of *scxa*⁺ cells indicated that decreased proliferation does not hamper atorvastatin-mediated *scxa* expansion. (H,I) Red bars indicate mean; individual points represent values for individual embryos; Mann-Whitney-Wilcoxon test. N.S., no significance; * $P<0.05$; ** $P<0.01$; **** $P<0.0001$. Representative craniofacial domain analyzed is shown in A-B',D-G. Ventral (A-B',D-G) views, anterior towards the left.

Statin increases the number of *scxa*-positive tendon cells derived from CNC skeletal progenitors

As increased proliferation cannot explain the statin-mediated tendon cell expansion, we explored the possibility that cells from adjacent tissues are recruited to tendon fates following statin treatment. In the craniofacial region, skeletal and tendon cells arise from the CNC and interact with the pharyngeal mesoderm-derived muscle to form the craniofacial musculoskeletal system (Chen and Galloway, 2014; Schilling and Kimmel, 1994). To determine whether statin alters musculoskeletal development, we examined muscle and cartilage tissues by whole-mount *in situ* hybridization. Atorvastatin treatment from 32 to 56 hpf altered the spatial expression patterns of *sox9a* (Fig. 3A,B), an early marker of skeletal progenitors and differentiating chondrocytes, *col2a1* (Fig. 3C,D), a component of the cartilage matrix (Yan et al., 2002), and *myod1* (Fig. 3E,F), a marker of myoblast progenitors (Lin et al., 2006). Specifically, the expression of *col2a1* (Fig. 3C,D, arrows) and *myod1* (Fig. 3E,F,

white arrow) appear to mark groups of cells that are not properly organized in the midline compared with controls. In the pectoral fin, the expression of *sox9a*, *col2a1*, *sox10:eGFP* and *myod1* (Fig. S4A-H) was present, but with an altered morphology following statin treatment. Quantification by qPCR showed increased expression of *sox9a* and *myod1* and no significant effect on *col2a1* expression (Fig. 3G). Together, these results suggest that statin alters the morphology of the forming cartilage and muscle but does not cause a loss in their respective gene expressions.

To further quantify the effects of statin on the numbers of chondrocyte and tendon cells, we performed flow cytometry on dissociated *Tg(scxa:mcherry;col2a1a:eGFP)* embryos treated with DMSO or statin (Dale and Topczewski, 2011). Consistent with our *col2a1* whole-mount *in situ* hybridization results, the morphology of *col2a1a:eGFP*⁺ cranial chondrocytes appeared altered (Fig. 3H-I') compared with controls. Using flow cytometry, we were able to identify singly positive *col2a1a*:

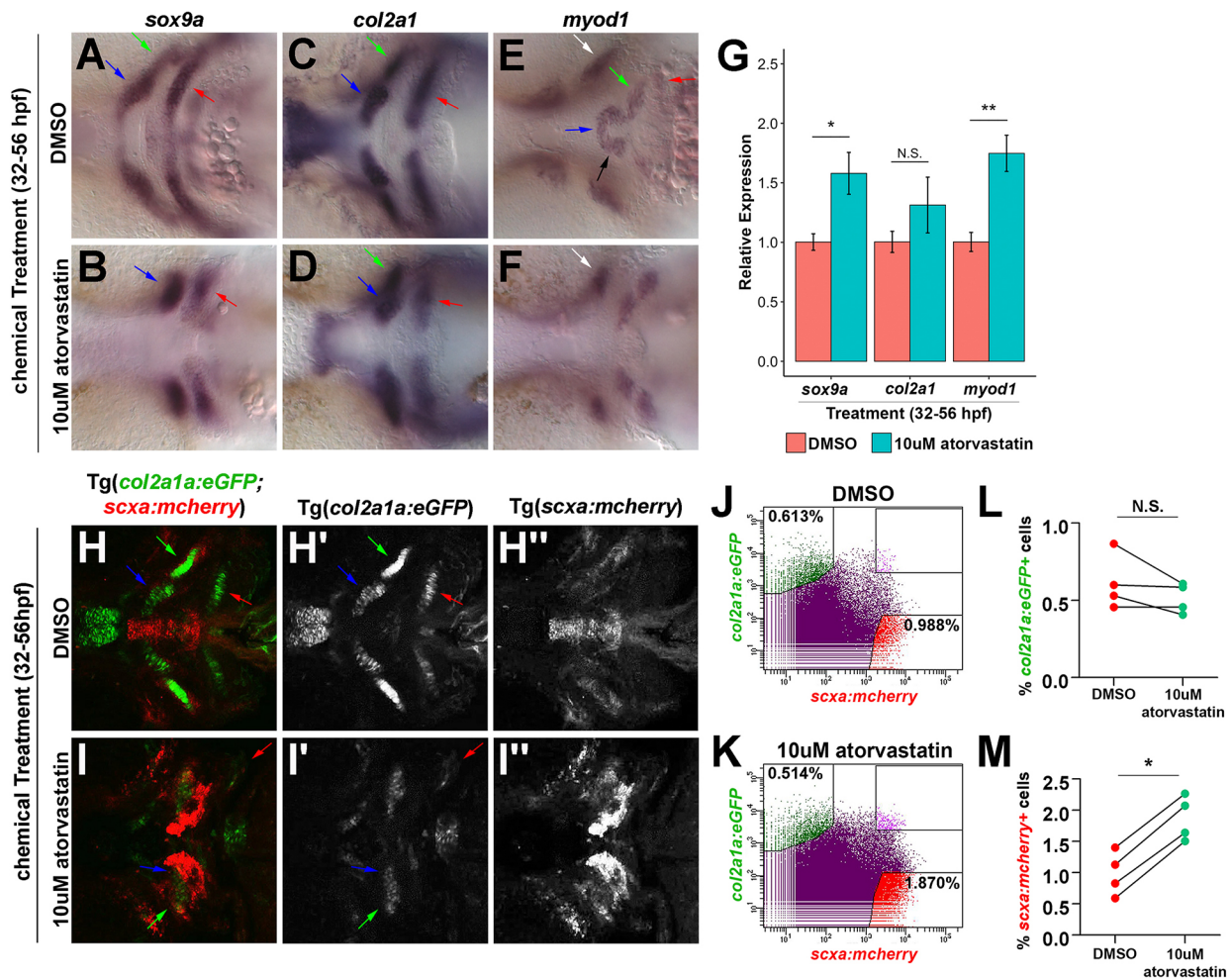


Fig. 3. Effect of statin on the craniofacial musculoskeleton. (A-F) Craniofacial expression of *sox9a*, *col2a1* and *myod1* at 56 hpf upon incubation from 32 to 56 hpf. At 56 hpf, atorvastatin altered the spatial expression patterns of *sox9a* (A,B), *col2a1* (C,D) and *myod1* (E,F) compared with controls. Arrows in A-D, H-I' mark Meckel's cartilage (blue), palatoquadrate cartilage (green) and ceratohyal cartilage (red). Arrows in E,F mark intermandibular anterior (blue), intermandibular posterior (black), hyohyal (green), interhyal (red) and adductor mandibularis (white). (G) qPCR quantification revealed that atorvastatin increased *sox9a* and *myod1* expression, but not *col2a1* at 56 hpf after incubation from 32 to 56 hpf compared with controls. $n=3$, whole embryo, Welch's two-tailed t -test. Data are mean \pm s.d. (H,I) Craniofacial expression of *col2a1a:eGFP*; *scxa:mcherry* at 56 hpf upon incubation from 32 to 56 hpf. Corresponding views of *eGFP* (H',I') and *mcherry* (H'',I''). (J,K) Representative flow cytometry analysis of *mcherry*⁺ tendon and *eGFP*⁺ cartilage cells at 56 hpf in the head region of Tg(*scxa:mcherry*; *col2a1a:eGFP*) embryos after incubation from 32 to 56 hpf. Atorvastatin expanded *mcherry*⁺ tendon progenitors (0.988% in DMSO; 1.870% in atorvastatin). (L,M) Flow cytometry quantification of *eGFP*⁺ and *mcherry*⁺ cells at 56 hpf in the head region of Tg(*scxa:mcherry*; *col2a1a:eGFP*) embryos after incubation from 32 to 56 hpf. Atorvastatin increased *mcherry*⁺ cells but not *eGFP*⁺ cells ($n=4$; Mann-Whitney-Wilcoxon test). N.S., no significance; * $P<0.05$; ** $P<0.01$. Ventral views (A-F, H-I'), anterior towards the left.

eGFP⁺ or *scxa:mcherry*⁺ cell populations from dissociated transgenic embryos. Statin had no effect on the percentage of *col2a1a:eGFP*⁺ cells, but significantly increased the percentage of *scxa:mcherry*⁺ cells (Fig. 3J-M). This approximate 2-fold expansion corresponds to the increase detected by qPCR and cell quantification analysis of stained embryos. Although a *scxa:mcherry*⁺/*col2a1a:eGFP*⁺ cell population was found in controls, this represented less than 0.1% of the total cells and changes to this population upon statin treatment were not statistically significant.

We next tested whether the increased craniofacial *scxa*⁺ cells of statin-treated embryos derive from the neural crest. We used expression of the Tg(*sox10:kaede*) (Dougherty et al., 2012) as a reporter to mark cells derived from the *sox10:kaede*⁺ lineage. Confocal images of craniofacial region of DMSO-treated ($n=4$ per timepoint) and atorvastatin-treated ($n=8$ per timepoint) embryos were analyzed for colocalized Kaede and *scxa* expression. By

analyzing the optical sections from confocal images, we found that *scxa*⁺ cells co-expressed the Kaede protein in all Tg(*sox10:kaede*) embryos examined following DMSO and atorvastatin treatment from 32 to 56 hpf (Fig. S4I-L). This demonstrates that the statin-mediated expanded *scxa*⁺ domain in the craniofacial region is exclusively derived from the CNC. Given the significant increase in *scxa*⁺ cells and expression in the craniofacial region, we focused on the craniofacial tendons in subsequent analyses.

Previous studies using genetic lineage tracing in mice have shown that tendon and ligament cells are descendants of *Sox9*⁺ cells (Huang et al., 2019; Soeda et al., 2010). Zebrafish *sox9a* marks migrating CNC as well as later skeletal cell types (Yan et al., 2005). Therefore, we sought to explore the possibility that the statin phenotype results from more CNC *sox9a*⁺ progenitors being diverted to *scxa*⁺ tendon fates. As our results show statin increases *sox9a* transcripts (Fig. 3G), we wanted to determine whether the expanded *scxa*⁺ cells co-expressed *sox9a*. To examine

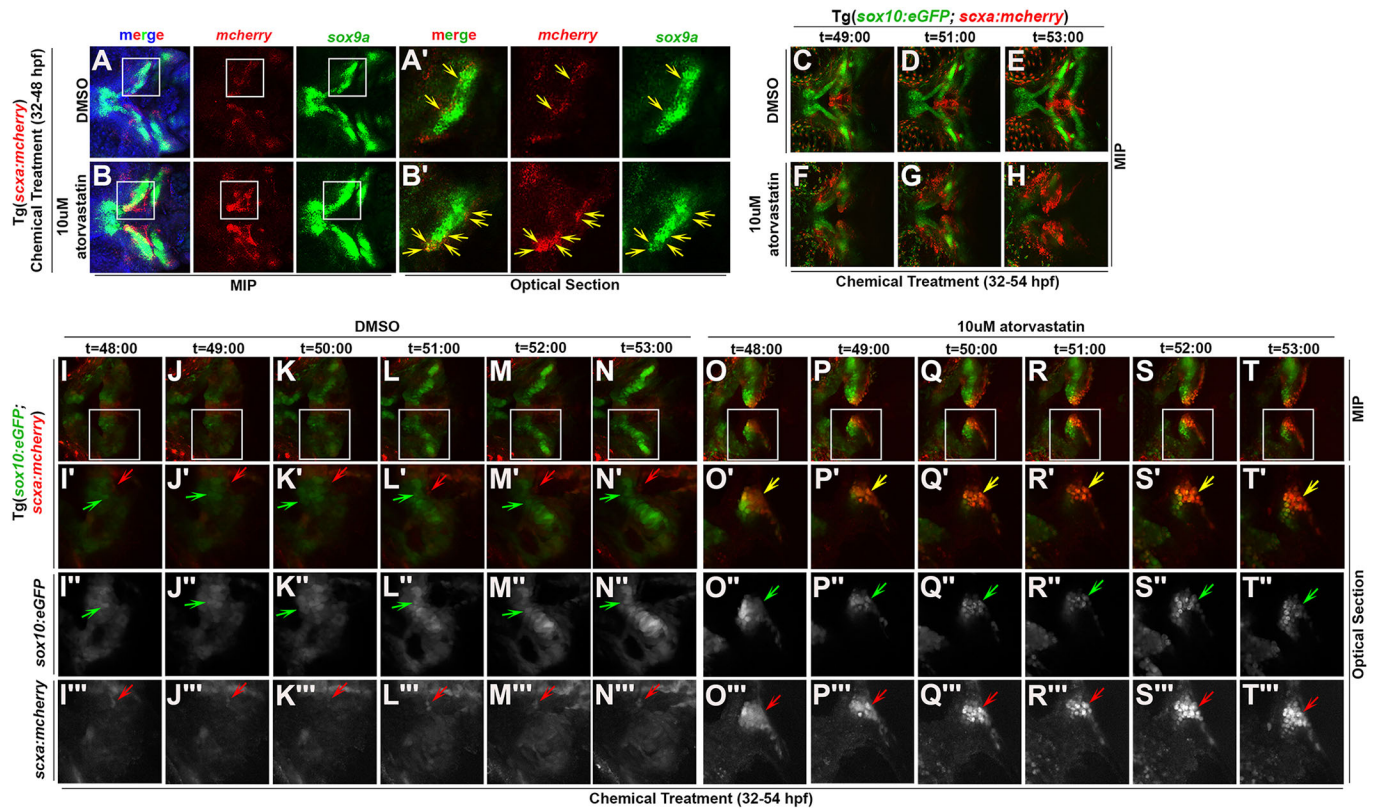


Fig. 4. Statin expands the *scxa*-expressing cell population by promoting tenogenic specification of CNC. (A-B') Expression of *mcherry* and *sox9a* in (A,A') DMSO and (B,B') atorvastatin-treated Tg(*scxa:mcherry*) embryos at 48 hpf. White boxes mark the craniofacial domain in maximum intensity projection (MIP) (A,B), magnified in corresponding optical sections (A',B'). Yellow arrows mark *mcherry*⁺/*sox9a*⁺ cells. Atorvastatin expanded *mcherry*⁺/*sox9a*⁺ cells (B', compare with A'). (C-T'') Time-course of live imaging of tendon and cartilage development in (C-E,I-N'') DMSO- and (F-H,O-T'') atorvastatin-treated Tg(*sox10:eGFP;scxa:mcherry*) embryos (*n*=4 shown). Arrows mark *sox10:eGFP*⁺ cells of Meckel's cartilage (green), *scxa:mcherry*⁺ tendon progenitors (red) and *scxa:mcherry*⁺/*sox10:eGFP*⁺ cells (yellow). Atorvastatin expanded *scxa:mcherry*⁺/*sox10:eGFP*⁺ cells near the region where Meckel's cartilage forms (compare F-H and O-T'') with C-E and I-N''). White boxes mark the craniofacial domain in the MIPs (I-T) of high-resolution images, magnified in the corresponding MIPs (I'-T') and optical sections: eGFP (I''-T'') and *mcherry* (I'''-T''') expression. Ventral views, anterior towards the left.

co-expression of *scxa* and *sox9a*, we performed fluorescent whole-mount *in situ* hybridization for transcripts of *sox9a* and *mcherry* for identifying *scxa:mcherry*⁺ tendon progenitors. For most regions in the lower jaw, *sox9a* and *mcherry* occupied spatially distinct domains in DMSO-treated Tg(*scxa:mcherry*) embryos at 48 hpf. In these control embryos, limited co-expression of *mcherry* and *sox9a* in some tendon attachment regions, specifically near the forming palatoquadrate and maxilla were observed (Fig. 4A,A', yellow arrows). In contrast, we observed significant and consistent co-expression of *sox9a* and *mcherry* in statin-treated Tg(*scxa:mcherry*) embryos at 48 hpf (Fig. 4B,B', yellow arrows).

sox9a and *sox10:eGFP* are expressed in CNC cells by 26 hpf, but their later expression becomes predominantly restricted to the forming cartilage elements by 48 hpf (Carney et al., 2006; Yan et al., 2005). Based on this, we wanted to determine whether statin causes *sox10:eGFP*⁺ CNC progenitors to adopt a tendon fate. To test this possibility, we performed live imaging of Tg(*scxa:mcherry; sox10:eGFP*) embryos treated with DMSO or statin from 32 to 53 hpf. Analysis of live images shows *sox10:eGFP*⁺ cells in and around Meckel's cartilage co-expressing *scxa:mcherry* in statin-treated embryos (Fig. 4F-H,O-T''), arrows) whereas this was not observed in controls (Fig. 4C-E,I-N''), arrows). Taken together, these results indicate that the statin-mediated increase in *scxa*⁺ cranial tendon cells results from the conversion of CNC *sox9a*⁺/*sox10*⁺ progenitors to *scxa*⁺ cells.

The effect of statin on patterning and known tendon-promoting signaling pathways

One potential mechanism by which multipotent CNC cells might be diverted to a different cell fate would be if the patterning of the craniofacial region were altered. To test this, we examined known markers of anterior-posterior and dorsal-ventral arch polarity. Despite statin-mediated *scxa* expansion (Fig. S5A,B), we did not identify any major patterning alterations in the expression of *hoxa2b*, *hoxb2a*, *hand2*, *bapx1*, *shha*, *patched1* or *gsc* at the stages examined (Hunter and Prince, 2002; Miller et al., 2003), although the expression levels of some genes appeared reduced upon chemical treatment compared with controls (Fig. S5C-M,R). This suggested that dorsal-ventral and anterior-posterior arch polarity are not affected by statin. A second possibility was that statins could interact with and act through pathways known to maintain or promote tendon fate. We interrogated constituents of the BMP (*bmp4*), TGFβ (*tgfb2a* and *tgfb1*), FGF (*pea3*) and Wnt (*fzd7a* and *fzd7b*) pathways (Brent and Tabin, 2004; Pryce et al., 2009; ten Berge et al., 2008; Yamamoto-Shiraishi and Kuroiwa, 2013), and observed no increase in expression of any markers in atorvastatin-treated embryos compared with controls (Fig. S5N-Q,S-X). Analysis of embryos transgenic for *6xTcf/Lef3S-miniP:d2eGFP* (Shimizu et al., 2012) and *bre:egfp* (Laux et al., 2011), which mark Wnt/β-catenin-mediated Tcf and BMP/Smad1/5 transcriptional activity, respectively, did not show expanded *egfp* expression in

atorvastatin-treated embryos compared with controls (Figs S5Y-B' and S6A-F). Although some differences in *bre:egfp* expression were observed near the mouth and posterior pharyngeal arch regions of statin-treated embryos, these alterations are consistent with a developmental delay in *bre:egfp* expression based on previous descriptions (Laux et al., 2011). To examine TGF β signaling and its interaction with the statin-mediated *scxa* expansion, we treated embryos with an ALK5 inhibitor (SB-431542) (Inman et al., 2002), alone and in combination with atorvastatin. We found SB-431542 significantly decreased *scxa* expression and increased *sox9a* expression at 56 hpf compared with controls (Fig. S6G). In embryos co-treated with SB-431542 and atorvastatin, *scxa* expression is significantly increased compared with SB-431542 treatment alone to a level comparable to that of DMSO controls. The finding that statin rescues *scxa* expression in the presence of TGF β inhibition suggests that the pathway targeted by statin acts independently of TGF β signaling. Furthermore, we performed staining for phospho-Smad3 and observed differences in phospho-Smad3 staining surrounding the cartilage regions of statin-treated embryos compared with controls. Although this result indicates altered TGF β signaling in statin-treated embryos, these phospho-Smad3⁺ regions did not co-express *scxa:mcherry* (Fig. S6H-S'). Together, these results suggest that statin may alter the activity of some signaling pathways in the craniofacial region, but it is unclear how these changes could directly cause the increase in tendon cells.

Inhibition of Hmgcr and mevalonate production expands the craniofacial tendon program

Taken together, our results suggest that statins expand the progenitor pool by altering CNC cell specification through a pathway previously unexplored in this context. To confirm the chemical inhibition results, we established that the expanded tendon cell phenotype results from statin inhibition of Hmgcr, the rate-limiting enzyme of the mevalonate pathway (Fig. 5A). Zebrafish have two HMGCR orthologs, *hmgcra* and *hmgcrb*. *hmgcra* is expressed in the larval liver and intestine; *hmgcrb* is maternally transcribed and ubiquitously expressed during early development (Thorpe et al., 2004). As *hmgcrb* is expressed during the spatial-temporal domain of interest, we focused on *hmgcrb* for further analysis. To test whether the statin-mediated expansion in craniofacial tendon progenitors is due to inhibition of Hmgcrb, we examined *scxa* and *colla2* expression in *hmgcrb*-deficient embryos by whole-mount *in situ* hybridization. In the *hmgcr1b*^{S617} mutants (D'Amico et al., 2007; Mapp et al., 2011), identified by their severe pericardial edema, *scxa* expression appears expanded at 60 hpf, and in a subset at 76 hpf, the pattern of *colla2* is expanded compared with controls (Fig. S7A-D, arrow). The remaining mutants had extreme morphological abnormalities and did not express *colla2*. Morpholino-mediated knockdown of the maternal and zygotic *hmgcrb* in zebrafish resulted in severe morphological defects and death prior to the onset of craniofacial *scxa* expression. Consistent with the zebrafish phenotype, the *Hmgcr* knockout in mouse is embryonic lethal (Ohashi et al., 2003), suggestive of an essential role for HMGCR/Hmgcr in early mouse and zebrafish development. For this reason, we injected a sub-lethal concentration of morpholino directed against *hmgcrb*. We next exposed the same sensitized embryos to a dose of atorvastatin that alone does not cause a tendon phenotype from 32 to 56 hpf. In this manner, we were able to induce loss of Hmgcrb within a specified developmental time window and to circumvent its earlier embryonic requirement. We observed an expansion of *scxa* in

such doubly treated embryos at 56 hpf compared with controls (Fig. S7E-H, arrow), suggesting an essential role for Hmgcrb inhibition in the statin-mediated expansion of craniofacial *scxa*. To obtain unequivocal evidence that inhibition of the mevalonate pathway is responsible for the phenotype observed, we rescued the expansion in craniofacial *scxa* expression to wild-type levels at 56 hpf with injection of mevalonic acid, the immediate metabolite targeted by statin (Fig. 5B-D). Together, these data establish the inhibition of Hmgcrb as the mechanism by which statin promotes expansion of craniofacial *scxa*⁺ tendon progenitors in the zebrafish.

Statin promotes the craniofacial tendon program through inhibition of Rac GTPases

The mevalonate pathway metabolizes the biosynthesis of cholesterol and isoprenoids (Goldstein and Brown, 1990). Isoprenoids are covalently attached to proteins by post-translational farnesylation or geranylgeranylation. Farnesylation is the addition of CaaX by farnesyltransferase (FTase); geranylgeranylation is the addition of CAAL by geranylgeranyltransferase I (GGTase I) or GGTase II (McTaggart, 2006). To test the requirement of the cholesterol and/or prenylation branches of the mevalonate pathway in *scxa* expansion, we incubated embryos with inhibitors of GGTase I (GGTI-286) (Lerner et al., 1995), FTase (FTI-277) (Lerner et al., 1995) and 2,3-oxidosqualene:lanosterol cyclase (Osc; RO48-8071) (Morand et al., 1997). Inhibition of all three branches in combination causes *scxa* expansion at 56 hpf, which phenocopies that of embryos treated with atorvastatin alone (Fig. S7I,K, arrow). Conversely, microinjection of farnesyl pyrophosphate, a branch-point intermediate for the cholesterol and prenylation branches, rescued *scxa* expression at 56 hpf following atorvastatin treatment (Fig. 5E).

To dissect the pathways involved in the statin-mediated tendon cell expansion, we targeted specific branches of the mevalonate pathway using genetic and chemical loss- and gain-of-function approaches. To test the requirement of the prenylation branch in the expansion of *scxa*, we knocked down essential regulators of prenylation, *FTase beta* (*fnfb*) and *protein GGTase I beta* (*pggt1b*) (Mapp et al., 2011). We found that loss of both *fnfb* and *pggt1b* resulted in an expansion of craniofacial *scxa* at 60 hpf compared with controls (Fig. 5G,H), suggesting that inhibition of prenylation sufficiently expands craniofacial *scxa* expression. This expansion of *scxa* is found in *pggt1b* morphants alone (Fig. 5I), whereas *scxa* is reduced in *fnfb* morphants (Fig. 5J), indicating that loss of GGTase I can elicit a tendon cell expansion. Furthermore, microinjection of geranylgeranyl pyrophosphate, an intermediate unique to the geranylgeranylation branch (McTaggart, 2006), rescued *scxa* expression at 56 hpf following atorvastatin treatment (Fig. 5F). To completely exclude the possibility that the cholesterol branch could be involved in expanding *scxa* expression, we inhibited cholesterol production. We found RO48-8071 had no significant effect on *scxa*, *sox9a* and *myod1* transcripts, and significantly decreased *col2a1* expression at 56 hpf compared with controls (Fig. 5K), suggesting that inhibition of the cholesterol biosynthesis branch does not expand craniofacial *scxa*⁺ tendon progenitors. Together, our data indicate that inhibition of geranylgeranylation alone and GGTase I specifically is required for the statin-mediated expansion of craniofacial *scxa*⁺ tendon progenitors in zebrafish.

GGTase I catalyzes the geranylgeranylation of the Rho family of GTPases, regulators of extracellular signaling that control actin cytoskeleton organization, transcriptional activation and mitogenesis (McTaggart, 2006). We examined the role of the Rho family members (Rho, Rac and Cdc42) in patterning the

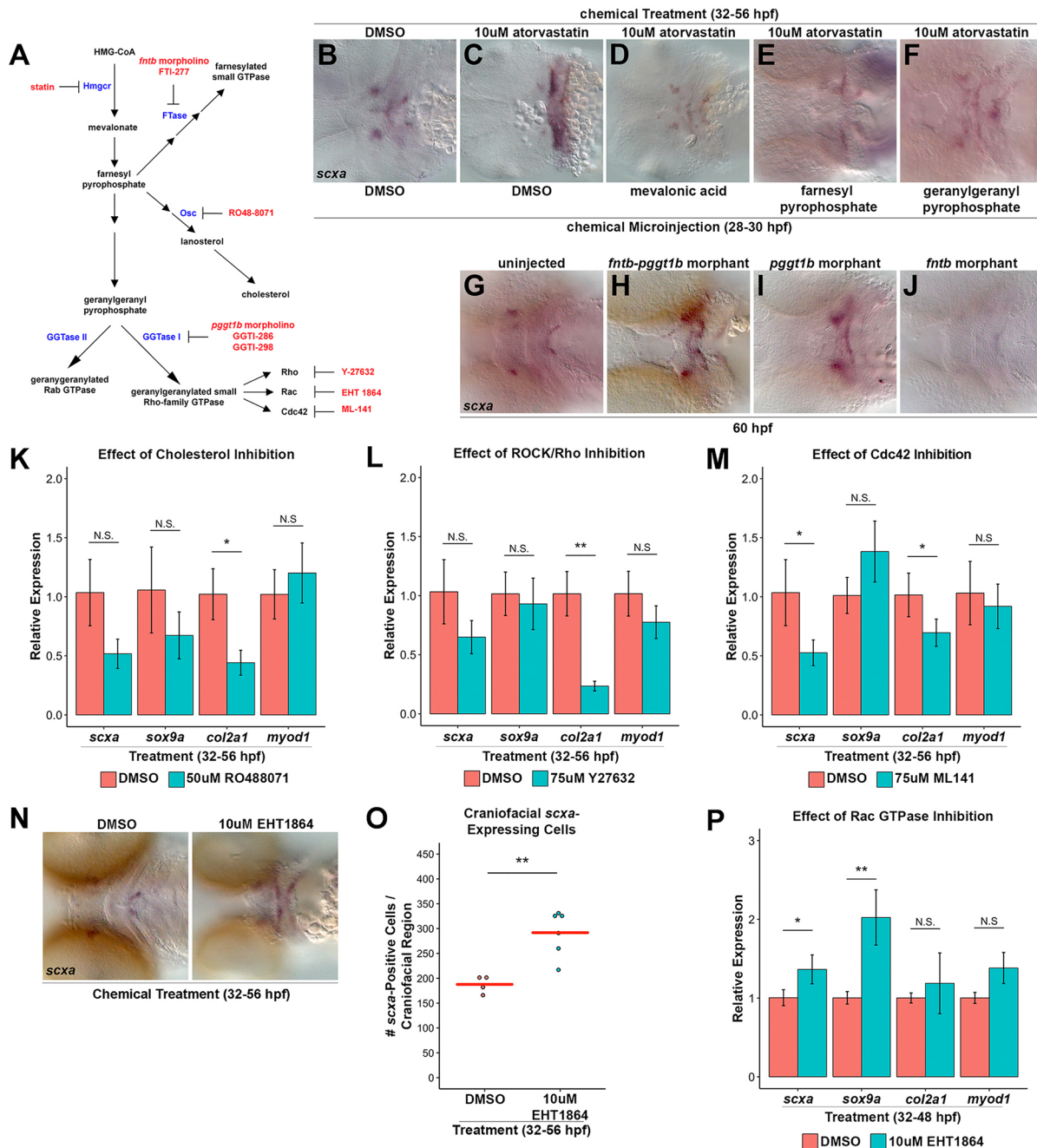


Fig. 5. Inhibition of geranylgeranylation branch causes statin-mediated tendon cell expansion. (A) Schematic of Hmgcr pathway with enzymes (blue), inhibitors (red) and morpholinos (red) indicated. (B,C) *scxa* expression in control DMSO-treated/DMSO-injected embryos at 56 hpf (B, 100%; n=30) is expanded upon atorvastatin treatment and DMSO injection (C, 100%; n=62). (D-F) *scxa* expression is rescued to wild-type levels in embryos incubated with atorvastatin from 32 to 56 hpf and injected at 28 hpf with mevalonic acid (D, 94% rescued; n=18), farnesyl pyrophosphate (E, 33% rescued; n=72) or geranylgeranyl pyrophosphate (F, 49% rescued; n=43). (G-J) At 60 hpf, craniofacial *scxa* expression, compared with controls (G, 100% wild type, n=41), is expanded in *fntb-pggt1b* morphants (H, 73% expanded, n=103) and *pggt1b* morphants (I, 60% expanded, n=89), and reduced in *fntb* morphants (J, 29% reduced; n=17). (K-M) qPCR analysis of *scxa*, *sox9a*, *col2a1* and *myod1* expression at 56 hpf after incubation from 32 to 56 hpf. (K) Cholesterol biosynthesis inhibition (using RO48-8071) reduced *col2a1*, but had no effect on *scxa*, *sox9a* and *myod1* compared with controls. (L) ROCK/Rho inhibition (using Y-27632) reduced *col2a1*, but had no effect on *scxa*, *sox9a* and *myod1* compared with controls. (M) Cdc42 GTPase inhibition (using ML-141) reduced *scxa* and *col2a1*, but did not affect *sox9a* and *myod1*. (N) Rac GTPase inhibition (using EHT-1864) expanded *scxa* expression at 56 hpf after incubation from 32 to 56 hpf. (O) EHT-1864 increased the quantity of *scxa*⁺ cells at 56 hpf after incubation from 32 to 56 hpf. (P) qPCR analysis of *scxa*, *sox9a*, *col2a1* and *myod1* expression at 56 hpf after incubation from 32 to 56 hpf. EHT-1864 increased expression of *scxa* and *sox9a*, but did not affect *col2a1* and *myod1*. For qPCR (K-M,P), n=3, head region, Welch's two-tailed t-test. Data are mean±s.d. (O) Red bars indicate mean; points represent individual embryos; Mann-Whitney-Wilcoxon test. N.S., not significant; *P<0.05; **P<0.01. Ventral views (B-J,N), anterior towards the left.

craniofacial musculoskeletal tissues using chemical inhibitors specific to each pathway. ROCK/Rho inhibition (Y-27632) (Uehata et al., 1997) significantly reduced *col2a1*, while *scxa*,

sox9a and *myod1* were not significantly changed at 56 hpf (Fig. 5L). Cdc42 inhibition (ML-141) (Hong et al., 2013) significantly reduced *scxa* and *col2a1*, but had no significant effect on *sox9a*

and *myod1* expression at 56 hpf (Fig. 5M). In contrast, Rac GTPase inhibition (EHT-1864) (Shutes et al., 2007) caused a qualitative expansion of *scxa* expression by whole-mount *in situ* hybridization (Fig. 5N) and significant quantitative increase in *scxa*⁺ cells (Fig. 5O) at 56 hpf. Expression of *scxa* and *sox9a* was also significantly increased, whereas *col2a1* and *myod1* were not significantly altered by qPCR upon EHT-1864 treatment at 48 hpf (Fig. 5P). Therefore, the two processes observed upon statin treatment, the expansion of craniofacial *scxa*⁺ tendon progenitors and an increase in *sox9a* expression, can be reproduced through EHT-1864 inhibition of Rac GTPase activity. Although a similar morphological result from pathway inhibition may not represent a true phenocopy, we believe the similarity in gene expression changes caused by Rac inhibition strongly suggests that inhibition of mevalonate through Rac GTPases, results in *scxa* expansion.

DISCUSSION

The mechanisms underlying tendon progenitor specification in vertebrates have remained elusive. Although TGFβ and FGF can promote tendon differentiation, no major signaling pathways have been identified to regulate tendon induction (Brent et al., 2003; Pryce et al., 2009; Havis et al., 2016). The small-molecule screen described here identified a new pathway as a crucial regulator of this process. We propose that inhibition of Hmgcr expands the craniofacial tendon progenitor pool through recruitment of neighboring *sox9a*⁺ CNC cells, diverting them from a *sox10*:*eGFP*⁺ skeletal fate (Fig. 6). Moreover, our data suggest that the mevalonate pathway acts through Rac GTPases in this context, thereby implicating a unique role for the mevalonate pathway and Rac GTPases in the formation of CNC tendon progenitors.

Cranial neural crest lineage specification

CNC cells are a multipotent population (Le Douarin and Kalcheim, 1999), although the time at which these cells become restricted and cues directing the cells towards individual fates are not well understood. Subpopulations of the CNC were postulated to become limited in potential prior to their ventral migration (Le Douarin and Smith, 1988). However, other studies have demonstrated that migrating CNC cells contain both pluripotent and lineage-restricted populations when cultured *in vitro* (Baroffio et al., 1991). Consistent with these findings, CNC cell fates can be altered in response to different signaling environments, indicating the cells are more plastic than originally believed (Trainor and Krumlauf, 2000). A single cell profiling analysis of mouse neural crest cells showed that cell fate decisions are made through the sequential stages of co-activation of transcriptional programs of competing fates, followed by transcriptional biasing, and finally by resolution towards one of the fates (Soldatov et al., 2019). Within the mesenchymal lineage, the CNC contains osteo-chondrogenic progenitors that become segregated into two distinct fates, cells that give rise to the bones that form either by endochondral ossification or intramembranous ossification (Akiyama et al., 2005; Mori-Akiyama et al., 2003; Nakashima et al., 2002). These studies, along with *in vitro* differentiation experiments showing osteogenic and chondrogenic differentiation potential of cells derived from embryonic calvarial bone (Grigoriadis et al., 1990; Stringa and Tuan, 1996), support the existence of bi-potential CNC-derived skeletal progenitors. In our studies, we observe changes in *scxa*⁺, *scxa*⁺/*sox9a*⁺ and *scxa*⁺/*sox10*⁺ cells in embryos treated with statin after the completion of CNC ventral cell migration. Our results are consistent with a model in which the post-migratory CNC cells contain multipotent bone-

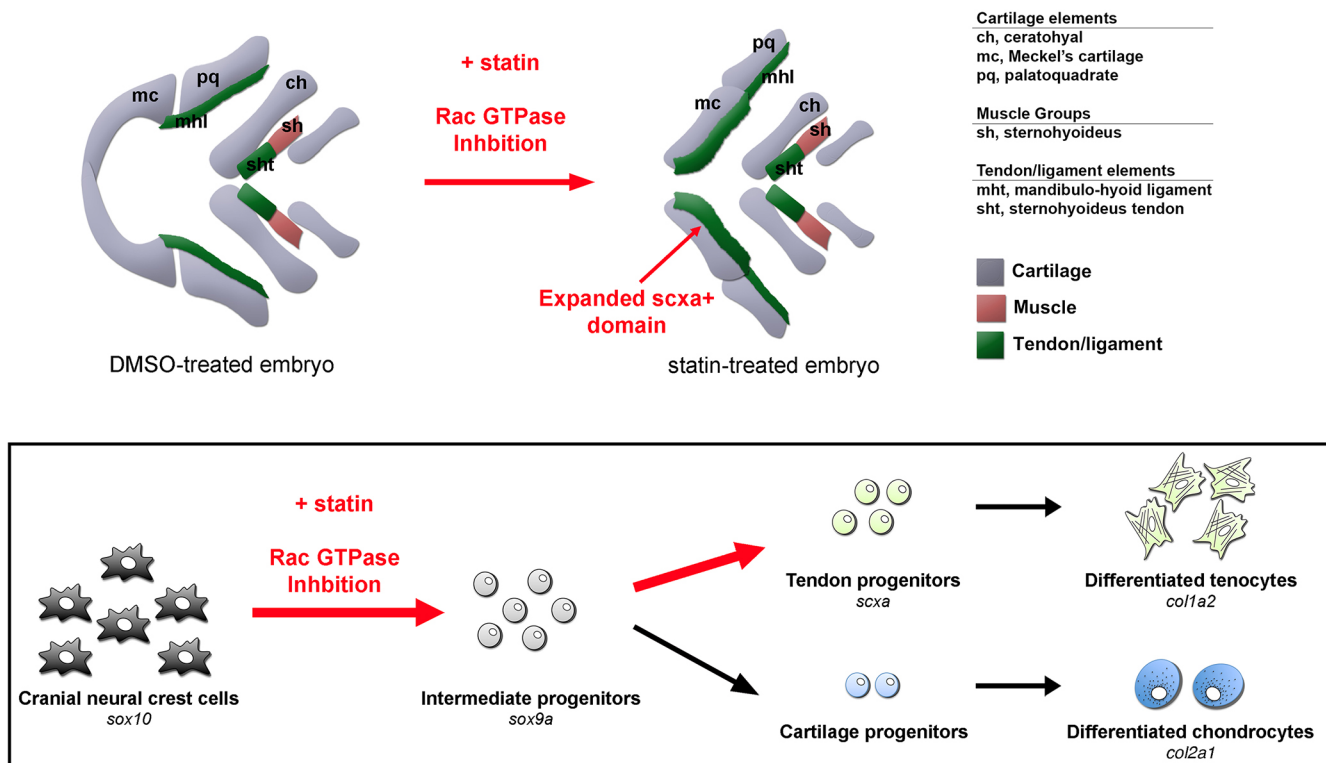


Fig. 6. Model for the mechanism of statin-mediated expansion of zebrafish craniofacial tendon program. Schematic illustrates selected craniofacial cartilage, muscle and tendon/ligament groups in ventral view of DMSO- and statin-treated zebrafish at 56 hpf after incubation from 32 to 56 hpf. Exposure of multipotential chondrocyte-tendon progenitors to statins results in re-specification towards a tendon fate – a process mediated through RAC GTPase inhibition. This cell fate expansion is spatially restricted to subsets of CNC-derived elements.

cartilage-tendon-forming progenitors rather than fate-restricted cells committed to one lineage. Studies have suggested that such multipotent progenitors capable of becoming ligament or bone exist in the zebrafish in a specific craniofacial region in the hyoid arch (Nichols et al., 2016). In our work, expression analysis of tendon markers revealed that the statin-mediated expansion of the craniofacial tendon program is localized to defined domains of the pharyngeal arches, as we never observed the entire skeletal-forming region converting to tendon fates. The restriction in the expansion of the tendon program indicates that either not all populations of CNC-derived mesenchyme are competent to activate a tendon program upon inhibition of the mevalonate pathway, or that skeletal-tendon progenitors are equivalent in their potential throughout the craniofacial region, but a subset of these sit in a microenvironment permissive for statin-mediated activation of tendon fates. These possibilities of cell competence to form tendon or site-specific signaling differences could explain why the axial tendon cells are not expanded upon statin treatment. In considering CNC tendon specification as it relates to other regions of tendon formation, cranial and limb/fin tendon progenitors have been previously suggested to have similar modes of regulation, as these regions do not require muscle for their specification whereas the axial tendon progenitors do (Brent et al., 2005; Edom-Vovard and Duprez, 2004; Grenier et al., 2009). Based on this, it is interesting to note that statin-mediated expansion of *scxa* expression was observed in fin and craniofacial regions, but not in axial locations. Further experiments are necessary to discern whether this represents a broader similarity in specification programs between the two regions.

Co-expression of *sox9a* and *scxa* in tendon development

In addition to increased numbers of *scxa*⁺ cells, our study demonstrates that statin promotes a broader *scxa*⁺/*sox9a*⁺ domain. Previous mouse lineage-tracing studies in the limb have shown that *Sox9*⁺ cells contribute to tendon tissues (Huang et al., 2019; Soeda et al., 2010). In the zebrafish head, *sox9a* and *sox10* are expressed throughout the post-migratory CNC cells at 26 hpf prior to the initiation of cranial *scxa* expression. Previous work and the lineage-tracing studies in this paper show that cranial *scxa*⁺ cells descend from a CNC *sox10* lineage. Therefore, it is likely that the cranial tendons also form from *sox9a*⁺ cells despite there being few *scxa*⁺ cells co-expressing either *sox9a* or *sox10* when *scxa* initiates expression after 40 hpf. This likely reflects the restriction in differentiation of these cells to *sox9a*⁺/*sox10*:*eGFP* cartilage or *scxa*⁺ tendon fates. We observe a few *scxa*⁺/*sox9a*⁺ cells located at tendon-bone interfaces for Meckel's adductor tendon and palatoquadrate adductor tendon (Fig. 4A-C', yellow arrow) (McGurk et al., 2017). The localization of *scxa*⁺/*sox9a*⁺ cells in wild-type embryos could indicate a similarity to the mammalian tendon-bone attachment unit, which also co-expresses these markers (Blitz et al., 2013; Sugimoto et al., 2013). Therefore, the statin-mediated increase in *scxa* and *sox9a* transcript levels along with a broadened *scxa*⁺/*sox9a*⁺ region could be interpreted in two ways: statin results in the persistent expression of *sox9a* and expansion of *scxa*, resulting in the conversion of CNC multipotent skeletal progenitors to tendon fates; or there is an increase in tendon-bone attachment unit cell types following statin treatment. We believe our data more strongly support the former interpretation, as our live imaging shows *sox10*:*eGFP*⁺ cells turning on *scxa*:*mcherry* expression upon statin treatment, which is not observed in wild-type embryos at this stage. In addition, we observe persistent expanded *scxa* expression upon statin treatment, whereas in mouse attachment units, *Scx* expression is not maintained at later stages of

development (Blitz et al., 2013). Although our live imaging could suggest a direct transdifferentiation event from *sox10*:*eGFP*-expressing chondrocytes to *scxa*:*mcherry*-expressing cells, we favor a model where statin mediates the conversion of multipotent *sox9a*⁺/*sox10*:*eGFP*⁺ progenitors to tendon fates prior to the initiation of *col2a1a*:*eGFP*. Consistent with this interpretation, we do not observe a decrease in *col2a1a*:*eGFP*⁺ cells or cartilage-associated transcripts (*col2a1*) by qPCR (Fig. 3). This interpretation is also consistent with single cell analysis of murine neural crest cells, showing co-activation of competing fate programs prior to the commitment to a specific cell fate (Soldatov et al., 2019). Notwithstanding, given that statin increases craniofacial *sox9a* expression (Fig. 3A,B,G) and we did not examine *col2a1* expression at later developmental stages, we cannot formally exclude the possibility that statin-mediated modulation of CNC cell fate specification may also direct cells towards a chondrocyte fate. We did observe abnormal cartilage morphology similar to previous reports of statin treatment (Signore et al., 2016). Altered *scxa* expression pattern was also observed for many of the chemical treatments, which could result from the chemicals targeting pathways associated with cell migration (Eisa-Beygi et al., 2014; Thorpe et al., 2004) and the cytoskeleton (Giger and David, 2017; Kardash et al., 2010; Xu et al., 2012). Interestingly, we found many of the expanded *scxa*-expressing cells within the periphery of the cartilage elements, corresponding to perichondrium, suggesting the expanded *scxa* cells arise from perichondrial cells. However, the lack of specific perichondrial markers prior to their morphological appearance makes it difficult to directly test this hypothesis.

Musculoskeletal development and the cytoskeleton

Despite the consistent statin-mediated increase in *scxa*⁺ cells, we observed differing results upon inhibition of branch points downstream in the mevalonate pathway. Inhibition of Rac GTPases alone could produce similar increases in *scxa* and *sox9a* transcripts, and had no significant effect on *col2a1* expression. In contrast, inhibition of cholesterol synthesis and ROCK/Rho GTPases had no significant effect on *scxa* and *sox9a* expression. Inhibition of cholesterol synthesis, ROCK/Rho or Cdc42 had a negative effect on *col2a1* expression. Consistent with our findings, conditional knockout of Cdc42 using *Prx1-Cre* resulted in abnormal chondrogenesis in mice (Aizawa et al., 2012). We also found that ML141-mediated inhibition of Cdc42 reduced *scxa* expression, whereas EHT1864-mediated inhibition of Rac increased *scxa* expression and quantity of *scxa*⁺ tendon progenitors (Fig. 5N-P), potentially indicating a binary relationship in which Cdc42 is required for and Rac restricts tenogenic fate. Our finding that Cdc42 inhibition reduces *scxa* expression is consistent with a requirement for Rho/ROCK signals in the expression of tendon markers in mammalian mesenchymal cells *in vitro* (Maharam et al., 2015).

Previous studies suggest a role for Rac signaling in regulating the cytoskeleton and cell-cell contacts during mesenchymal condensation, perhaps providing a permissive or restrictive environment for cell type specification (Woods et al., 2007). Condensation of mesenchymal progenitors is essential for cartilage formation and precedes their commitment to the chondrogenic lineage (DeLise and Tuan, 2002; Oberlender and Tuan, 1994). Indeed, cell morphology influences the differentiation of mesenchyme towards chondrogenic, osteogenic and adipogenic lineages (McBeath et al., 2004; Solursh et al., 1982). In tenocytes, cell morphology influences gene expression, such as that of collagen type I (Li et al., 2008; von der Mark et al., 1977), and the actin cytoskeleton functions in proper organization of the collagenous extracellular matrix (Canty et al., 2006). This model

suggests a cell-autonomous role for the mevalonate pathway and Rac GTPases in tendon fate regulation, but, as these pathways can affect multiple aspects of cell behavior and signaling, it is possible that the mevalonate pathway and Rac inhibition work indirectly on neighboring cells and tissues to alter unknown pathways that result in increased tendon specification events. Nevertheless, it is tempting to speculate that Rac inhibition results in a permissive signaling environment that directly or indirectly leads to mesenchymal progenitors adopting a tendon fate.

Conclusion

Using a zebrafish small-molecule screen, we established that the mevalonate pathway is involved in regulating specification of tenogenic fate based on expansion of a tendon marker domain. Our analyses of the cellular processes governing tendon cell induction provide evidence that, besides cell migration and proliferation, the mevalonate pathway has an important role in specifying cell fate in a developing embryo. Furthermore, we propose that the emergence of the tendon lineage from a common progenitor population occurs through multipotent *sox9a*⁺/*sox10*⁺ progenitors and is mediated by inhibition of Rac activity. These results could significantly impact the field of regenerative medicine in guiding approaches aimed at generating tendon tissues *in vitro*. Ultimately, our studies highlight the advantages of the zebrafish system and chemical screening for discovering novel genetic pathways involved in developmental processes.

MATERIALS AND METHODS

Zebrafish husbandry

Zebrafish were staged and maintained as described previously (Kimmel et al., 1995; Westerfield, 2000). All experiments were approved by the HMS and MGH IACUC. *sox10:kaede* (Dougherty et al., 2012), *sox10:mcherry* (Kamel et al., 2013), *sox10:eGFP* (Curtin et al., 2011), *col2a1a:eGFP* (Dale and Topczewski, 2011), *6xTcf/LefBS-miniP:d2eGFP* (Shimizu et al., 2012) and *bre:egfp* (Laux et al., 2011) were used. *hmgcr1b*^{s617} was obtained from Masazumi Tada (University College London, UK) (D'Amico et al., 2007). The *scxa:mcherry* transgene was generated using a bacterial artificial chromosome (BAC) containing the entire *scxa* genomic locus (CHORI BACPAC Resources). Using constructs and protocols provided by Stefan Schulte-Merker and Koichi Kawakami (Bussmann and Schulte-Merker, 2011; Suster et al., 2011), *mcherry* was recombineered into the first exon of the *scxa* BAC (CH211 251g8) and *tol2* sites were introduced into the vector backbone. Properly targeted BACs were injected, embryos were raised to adults, and *scxa:mcherry*-expressing offspring were identified and raised to establish the line (fb301Tg).

Chemical screen design and validation testing

Wild-type stage-matched embryos were arrayed into 48-well plates (~10 embryos per well) of individual compounds and exposed from 32 to 56 hpf. The NINDS Custom Collection 2 library (1040 known bioactives) was obtained from the Institute of Chemistry and Chemical Biology, Longwood Screening Facility. The compounds were dissolved in DMSO and subsequently diluted in E3 buffer to a final concentration of ~13 μM. Each compound was screened in duplicate; DMSO and SU5402 were negative and positive controls, respectively. Whole-mount *in situ* hybridization for *scxa* expression was performed to assess craniofacial tendon progenitors. Qualitative scoring (number of embryos with altered *scxa* expression per number scored) was conducted using the following criteria: normal/unchanged, decreased/absent and increased. Annotations were recorded regarding any changes in the spatial domain of *scxa*. Most compounds (97.69%; 1016/1040) failed to alter *scxa* expression, although two (0.19%) were toxic and resulted in death, 10 (0.96%) resulted in developmental delay and unaltered *scxa* expression, three (0.29%) resulted in general and non-specific morphological abnormalities, two (0.29%) increased *scxa* expression, six compounds were commercially unavailable and therefore could not be validated, and one (0.10%) decreased *scxa* expression.

qPCR of embryonic zebrafish

Whole zebrafish embryos (*n*=15-125) were collected at 56 hpf following atorvastatin treatment (32-56 hpf) and dissected craniofacial regions of zebrafish embryos (*n*=15-45) were collected at 48 hpf following EHT-1864 treatment (32-48 hpf), at 56 hpf following RO488071, Y27632, ML141 or atorvastatin±SB-431542 treatments (32-56 hpf), and at 72 hpf following atorvastatin (48-72 hpf) or fluvastatin (32-48 hpf) treatments. Owing to high rate of toxicity, embryos collected following fluvastatin were confirmed to have a beating heart and increased *scxa:mcherry* expression using a dissecting microscope. Embryos were pooled per condition for RNA extraction (Qiagen, 74104). After DNase treatment (Qiagen, 79254), cDNA was synthesized (Roche, 04379012001; Invitrogen, 18091200 and Fisher Scientific, 18-091-050). For TaqMan Fast Universal gene expression assays (Applied Biosystems, 4352042), the FAM-dye probes used were: *scxa* (Dr03104896) and *β-actin* (Dr03432610). For Fast SYBR Green PCR assays (Applied Biosystems, 4385618), the primers used were: *scxa* forward, 5'-GGCGTCCAGTTACATCTCT-3'; *scxa* reverse, 5'-GTCTTTGCTCATTTCTCTGGTT-3'; *sox9a* forward, 5'-GGCCGACCAGTACCCGCACCTC-3'; *sox9a* reverse, 5'-GATTGCTCTGGCCGTTCTTCA-CC-3'; *col2a1* forward, 5'-TGCTGCAGGGCTCCAATGATGT-3'; *col2a1* reverse, 5'-CTGCGCCAATGTCCACTCCGAAC-3'; *myod1* forward, 5'-GAGGGAGAGGAGGCGACTGAGC-3'; *myod1* reverse, 5'-CTGACACGTTGGGCCCCATAAAATC-3'; *colla2* forward, 5'-GCCCGCTGGTA-AAGATGGTTCAA-3'; *colla2* reverse, 5'-ACGGCAAGTACGA-GCGGGGTTCT-3'; *β-actin* forward, 5'-GATGCCCTCGTGCTGTTT-TC-3'; *β-actin* reverse, 5'-TCTCTGTTGGCTTTGGGATTCA-3'.

No-reverse transcriptase controls were used for each sample. The ratio of the target transcript to *β-actin* reference was quantified and normalized to the control sample. Statistical analysis was conducted with significance defined as *P*≤0.05 (Welch's two-sample two-tailed *t*-test) and error bars represent standard deviation based on all technical replicates and all biological replicates.

Morpholino design, pharmacological treatment and microinjection

Morpholinos (Gene Tools) were injected as described previously: *fn1β* *ATG* (Mapp et al., 2011), *hmgcr1b* *ATG* (D'Amico et al., 2007) and *pggt1β* *ATG* (Mapp et al., 2011). Morpholino concentrations were: *fn1β* (1.4 ng alone and 2.1 ng in *fn1β*-*pggt1β* morphants); *pggt1β* (5.5 ng alone and 2.8 ng in *fn1β*-*pggt1β* morphants); and 1.0 ng *hmgcr1b*. Embryos were incubated in the following compounds: atorvastatin, lovastatin, fluvastatin, FTI-277 and SU5402 (Tocris Bioscience); simvastatin, aphidicolin and GGTI-286 (Sigma-Aldrich); and RO48-8071, EHT-1864, ML-141, Y-27632 and SB-431542 (Cayman Chemical). In the metabolite rescue experiments, the pharyngeal cavity was injected at 28-30 hpf with 1-2 nl of the following compounds (Sigma-Aldrich): 2.6 mM geranylgeranyl pyrophosphate, 10 mM farnesyl pyrophosphate, 1.0 M mevalonolactone and DMSO or ethanol (vehicle control).

Expression and proliferation analysis

Colorimetric whole-mount *in situ* hybridization was performed as described previously (Brent et al., 2003). Probes include *scxa* (AL923903 and AL921296), *colla2* (DY559926), *tnmd* (BC155615 and EV754577), *myod1* (BC078421), *sox9a* (Yan et al., 2005), *col2a1* (Yan et al., 1995), *runx2a* (Burns et al., 2002), *hoxa2b* (Kong et al., 2014), *hoxb2a* (Kong et al., 2014), *hand2* (Foote et al., 2016), *bapx1* (Kamel et al., 2013), *tgfb1* (CB361081), *tgfb2a* (Thisse et al., 2001), *pea3* (Münchberg et al., 1999), *fzd7a* (Kamel et al., 2013), *fzd7b* (Rochard et al., 2016), *shha* (Piotrowski and Nüsslein-Volhard, 2000), *patched1* (Lewis et al., 1999), *bmp4* (Gonzalez et al., 2000), *ednraa* (Nair et al., 2007) and *gsc* (Erter et al., 1998). Fluorescent whole-mount *in situ* hybridization and antibody staining were performed as described previously (Chen and Galloway, 2017). Primary antibodies were 1:100 anti-PSmad3 (Abcam, ab52903); 1:500 anti-kaede (MBL, PM012M); and 1:200 anti-phospho-Histone H3 (Millipore, 06-570). The sensitivity of the anti-kaede antibody marks the descendants of the *sox10:kaede*⁺ lineage that have turned off *sox10:kaede* expression. Secondary antibodies were 1:500 goat anti-mouse IgG2b-HRP (Southern Biotech); 1:200 donkey anti-rabbit Alexa Fluor 488 and 1:500 donkey anti-

rabbit IgG-HRP (Jackson ImmunoResearch Laboratories); 1:400 goat anti-mouse Alexa Fluor 488 (Invitrogen); and 1:400 donkey anti-rabbit Alexa Fluor 647 (Abcam). All images captured were of representative embryos for each condition.

Quantification of EdU (5-ethynyl-2'-deoxyuridine)-positive cells

Tg(*sox10:mcherry*) embryos were chemically treated at 32 hpf, pulsed with EdU for 20 min at 4 h or 5 h intervals, and chased with E3 buffer for 30 min prior to fixation. Embryos were counterstained with Hoechst33342 (Invitrogen). For quantification, we used confocal microscopy and counted the number of proliferative cells in optical sections spanning the depth of a defined craniofacial region of the embryos processed by Click-iT EdU Alexa Fluor 488 Imaging Kit (Invitrogen, C10337). Statistical analysis was conducted with significance defined as $P \leq 0.05$ (Welch's two-sample two-tailed *t*-test) and error bars are standard deviation.

Quantification of *scxa*-, *col1a2*- and PH3-expressing cells

For quantification of craniofacial *scxa*- and *col1a2*-expressing cells, we counted the number of cells in optical confocal sections spanning the area of the craniofacial region of embryos stained for the transcript of interest by fluorescent whole-mount *in situ* hybridization and counterstained with Hoechst33342. For quantification of pectoral fin and myoseptal *scxa*-expressing cells, we counted the number of *mcherry*⁺ cells in maximum-intensity projection images spanning the width of the pectoral fin or trunk region, respectively, of Tg(*scxa:mcherry*) embryos. For quantification of cells co-expressing *scxa* transcript and PH3 protein (Fig. S3I,L-Q), we counted the number of cells in optical sections spanning the depth of a defined region of the embryos processed by fluorescent whole-mount *in situ* hybridization and immunohistochemistry. Statistical analysis was conducted using the Mann-Whitney-Wilcoxon test with significance defined as $P \leq 0.05$.

Image analysis and live imaging

Embryos were imaged using a Zeiss AxioZoom V16 with ApoTome2 or Nikon Eclipse 80i, and images were acquired using Zeiss Zen or NIS Elements. Confocal time-course images were taken using a Nikon ECLIPSE Ti-E and confocal images were taken using a Zeiss LSM 710 NLO or Nikon ECLIPSE Ti-E. Confocal images were acquired with Zeiss Zen or ImageJ software using the maximum-intensity projection (MIP) feature applied to *z*-stacks and processed uniformly with Photoshop. Tg(*bre:egfp*), Tg(*scxa:mcherry*), Tg(*col2a1a:eGFP*; *scxa:mcherry*) and Tg(*6XTcf/LefBS-miniP:d2eGFP*) embryos were mounted in 0.8-1.0% low melting-point agarose (RPI, 9012-36-6) in E3 buffer. Embryos for live imaging were anesthetized with 0.015-0.2% tricaine in E3 buffer. Embryos, positioned with the ventral side of the head facing the objective, were imaged every 1 h using a *z*-stack module. Post-imaging, the embryos resumed normal development at 28.5°C in fresh E3 buffer.

Phospho-Smad3 staining

56 hpf embryos were fixed in 4% PFA overnight and then rinsed in PBST (PBS+0.15% Triton X-100) for 3×10 min at room temperature (RT). Embryos were next permeated in 20 µg/ml Proteinase K (Thermo Fisher Scientific, 507203027) for 25 min at room temperature and rinsed in PBST for 3×10 min. Afterwards, the embryos were blocked with 4% BSA (ThermoFisher Scientific, BP1605-100) in PBST for 2 h at room temperature and subsequently incubated with anti-Smad3 antibody overnight at 4°C. Embryos were washed with PBST for at least 2 h, with the PBST changed every 30 min, and then incubated with donkey anti-rabbit Alexa Fluor 647 overnight at 4°C. Hoechst (ThermoFisher Scientific, H3570) was added to the secondary antibody solution for nuclear staining.

Fluorescent whole-mount *in situ* hybridization

Fluorescent whole-mount *in situ* hybridization was performed as previously described (Chen and Galloway, 2017) using DIG- (Roche, 11277073910) and fluorescein- (Roche, 11685619910) labeled RNA probes against *sox9a* and *mcherry*. Probes were synthesized using Sp6 or T7 RNA polymerase (Roche, 10810274001 or 10881767001). Signals were visualized using a

TSA Plus Fluorescein Evaluation Kit (PerkinElmer, NEL741E001KT) and TSA Cyanine 5 Evaluation Kit (PerkinElmer, NEL705A001KT).

Flow cytometry

The Tg(*col2a1a:eGFP*; *scxa:mcherry*) embryos were treated with DMSO or atorvastatin from 32 to 56 hpf. At 56 hpf, 15-20 pooled heads from each group were collected for single cell dissociation as previously described (Bresciani et al., 2018). The ratio of each population: *scxa:mcherry*⁺ cells, *col2a1a:eGFP*⁺ cells and *scxa:mcherry*⁺/*col2a1a:eGFP*⁺ cells were analyzed using a BD FACS Aria 3 Cell Sorter equipped with ultraviolet, green and red lasers. Gates were set using positive (single transgene for *scxa:mcherry* and *col2a1a:eGFP*) and negative (wild-type) control cell populations.

Acknowledgements

We thank Caroline Shamu, Jennifer Smith, David Wrobel and Doug Flood, and personnel at the ICCB Longwood, for assistance and guidance with the screen. We are grateful to Jessica Lehoczky, Mor Grinstein, Heather Dingwall, the BIDMC and MGH Simches fish facilities, Trista North, Wolfram Goessling, and North and Goessling lab members.

Competing interests

J.W.C. is currently a full-time employee at Genentech and holds stocks in Roche.

Author contributions

Conceptualization: J.W.C., X.N., C.J.T., J.L.G.; Methodology: J.W.C., X.N., M.J.K., M.-T.N., J.L.G.; Formal analysis: J.W.C., X.N., M.J.K., J.L.G.; Investigation: J.W.C., X.N., M.J.K., M.-T.N., J.L.G.; Resources: C.J.T., J.L.G.; Data curation: J.W.C., J.L.G.; Writing - original draft: J.W.C., X.N., C.J.T., J.L.G.; Writing - review & editing: J.W.C., X.N., M.J.K., M.-T.N., C.J.T., J.L.G.; Visualization: J.W.C., X.N., J.L.G.; Supervision: C.J.T., J.L.G.; Project administration: J.L.G.; Funding acquisition: J.L.G.

Funding

This work was supported by the National Institutes of Health (HD03443 to C.J.T.; AR074541, HD069533 and DE024771), by awards from the Charles H. Hood Foundation and the Harvard Stem Cell Institute to J.L.G., and by a National Science Foundation Graduate Research Fellowship grant (DGE1144152 to J.W.C.). Deposited in PMC for release after 12 months.

Supplementary information

Supplementary information available online at <http://dev.biologists.org/lookup/doi/10.1242/dev.185389.supplemental>

References

- Aizawa, R., Yamada, A., Suzuki, D., Imura, T., Kassai, H., Harada, T., Tsukasaki, M., Yamamoto, G., Tachikawa, T., Nakao, K. et al. (2012). Cdc42 is required for chondrogenesis and interdigital programmed cell death during limb development. *Mech. Dev.* **129**, 38-50. doi:10.1016/j.mod.2012.02.002
- Akiyama, H., Kim, J.-E., Nakashima, K., Balmes, G., Iwai, N., Deng, J. M., Zhang, Z., Martin, J. F., Behringer, R. R., Nakamura, T. et al. (2005). Osteochondroprogenitor cells are derived from Sox9 expressing precursors. *Proc. Natl. Acad. Sci. USA* **102**, 14665-14670. doi:10.1073/pnas.0504750102
- Baroffio, A., Dupin, E. and Le Douarin, N. M. (1991). Common precursors for neural and mesectodermal derivatives in the cephalic neural crest. *Development* **112**, 301-305.
- Blitz, E., Sharir, A., Akiyama, H. and Zelzer, E. (2013). Tendon-bone attachment unit is formed modularly by a distinct pool of Scx- and Sox9-positive progenitors. *Development* **140**, 2680-2690. doi:10.1242/dev.093906
- Brand-Saber, B. and Christ, B. (2000). Evolution and development of distinct cell lineages derived from somites. *Curr. Top. Dev. Biol.* **48**, 1-42. doi:10.1016/S0070-2153(08)60753-X
- Brent, A. E. and Tabin, C. J. (2004). FGF acts directly on the somitic tendon progenitors through the Ets transcription factors Pea3 and Erm to regulate scleraxis expression. *Development* **131**, 3885-3896. doi:10.1242/dev.01275
- Brent, A. E., Schweitzer, R. and Tabin, C. J. (2003). A somitic compartment of tendon progenitors. *Cell* **113**, 235-248. doi:10.1016/S0092-8674(03)00268-X
- Brent, A. E., Braun, T. and Tabin, C. J. (2005). Genetic analysis of interactions between the somitic muscle, cartilage and tendon cell lineages during mouse development. *Development* **132**, 515-528. doi:10.1242/dev.01605
- Bresciani, E., Broadbridge, E. and Liu, P. P. (2018). An efficient dissociation protocol for generation of single cell suspension from zebrafish embryos and larvae. *MethodsX* **5**, 1287-1290. doi:10.1016/j.mex.2018.10.009

- Burns, C. E., DeBlasio, T., Zhou, Y., Zhang, J., Zon, L. and Nimer, S. D. (2002). Isolation and characterization of runxa and runxb, zebrafish members of the runt family of transcriptional regulators. *Exp. Hematol.* **30**, 1381-1389. doi:10.1016/S0301-472X(02)00955-4
- Bussmann, J. and Schulte-Merker, S. (2011). Rapid BAC selection for tol2-mediated transgenesis in zebrafish. *Development* **138**, 4327-4332. doi:10.1242/dev.068080
- Canty, E. G., Starborg, T., Lu, Y., Humphries, S. M., Holmes, D. F., Meadows, R. S., Huffman, A., O'Toole, E. T. and Kadler, K. E. (2006). Actin filaments are required for fibroblast-mediated collagen fibril alignment in tendon. *J. Biol. Chem.* **281**, 38592-38598. doi:10.1074/jbc.M607581200
- Carney, T. J., Dutton, K. A., Greenhill, E., Delfino-Machin, M., Dufourcq, P., Blader, P. and Keshel, R. N. (2006). A direct role for Sox10 in specification of neural crest-derived sensory neurons. *Development* **133**, 4619-4630. doi:10.1242/dev.02668
- Chen, J. W. and Galloway, J. L. (2014). The development of zebrafish tendon and ligament progenitors. *Development* **141**, 2035-2045. doi:10.1242/dev.104067
- Chen, J. W. and Galloway, J. L. (2017). Using the zebrafish to understand tendon development and repair. *Methods Cell Biol.* **138**, 299-320. doi:10.1016/bs.mcb.2016.10.003
- Corsini, A., Mazzotti, M., Raiteri, M., Soma, M. R., Gabbiani, G., Fumagalli, R. and Paoletti, R. (1993). Relationship between mevalonate pathway and arterial myocyte proliferation: in vitro studies with inhibitors of HMG-CoA reductase. *Atherosclerosis* **101**, 117-125. doi:10.1016/0021-9150(93)90107-6
- Couly, G. F., Coltey, P. M. and Le Douarin, N. M. (1993). The triple origin of skull in higher vertebrates: a study in quail-chick chimeras. *Development* **117**, 409-429.
- Curtin, E., Hickey, G., Kamel, G., Davidon, A. J. and Liao, E. C. (2011). Zebrafish *wnt9a* is expressed in pharyngeal ectoderm and is required for palate and lower jaw development. *Mech. Dev.* **128**, 104-115. doi:10.1016/j.mod.2010.11.003
- Dale, R. M. and Topczewski, J. (2011). Identification of an evolutionarily conserved regulatory element of the zebrafish *col2a1a* gene. *Dev. Biol.* **357**, 518-531. doi:10.1016/j.ydbio.2011.06.020
- D'Amico, L., Scott, I. C., Jungblut, B. and Stainier, D. Y. R. (2007). A mutation in zebrafish *hmgcr1b* reveals a role for isoprenoids in vertebrate heart-tube formation. *Curr. Biol.* **17**, 252-259. doi:10.1016/j.cub.2006.12.023
- DeLise, A. M. and Tuan, R. S. (2002). Alterations in the spatiotemporal expression pattern and function of N-cadherin inhibit cellular condensation and chondrogenesis of limb mesenchymal cells in vitro. *J. Cell. Biochem.* **87**, 342-359. doi:10.1002/jcb.10308
- Dougherty, M., Kamel, G., Shubinets, V., Hickey, G., Grimaldi, M. and Liao, E. C. (2012). Embryonic fate map of first pharyngeal arch structures in the *sox10*: *kaede* zebrafish transgenic model. *J. Craniofac. Surg.* **23**, 1333-1337. doi:10.1097/SCS.0b013e31826f020b
- Edom-Vovard, F. and Duprez, D. (2004). Signals regulating tendon formation during chick embryonic development. *Dev. Dyn.* **229**, 449-457. doi:10.1002/dvdy.10481
- Eisa-Beygi, S., Ekker, M., Moon, T. W., Macdonald, R. L. and Wen, X.-Y. (2014). Developmental processes regulated by the 3-hydroxy-3-methylglutaryl-CoA reductase (HMGCR) pathway: highlights from animal studies. *Reprod. Toxicol.* **46**, 115-120. doi:10.1016/j.reprotox.2014.04.001
- Erter, C. E., Solnica-Krezel, L. and Wright, C. V. E. (1998). Zebrafish nodal-related 2 encodes an early mesodermal inducer signaling from the extraembryonic yolk syncytial layer. *Dev. Biol.* **204**, 361-372. doi:10.1006/dbio.1998.9097
- Footo, A. D., Vijay, N., Ávila-Arcos, M. C., Baird, R. W., Durban, J. W., Fumagalli, M., Gibbs, R. A., Hanson, M. B., Korneliusen, T. S., Martin, M. D. et al. (2016). Genome-culture coevolution promotes rapid divergence of killer whale ecotypes. *Nat. Commun.* **7**, 11693. doi:10.1038/ncomms11693
- Giger, F. A. and David, N. B. (2017). Endodermal germ-layer formation through active actin-driven migration triggered by N-cadherin. *Proc. Natl. Acad. Sci. USA* **114**, 10143-10148. doi:10.1073/pnas.1708116114
- Goessling, W. and North, T. E. (2014). Repairing quite swimmingly: advances in regenerative medicine using zebrafish. *Dis. Model. Mech.* **7**, 769-776. doi:10.1242/dmm.016352
- Goldstein, J. L. and Brown, M. S. (1990). Regulation of the mevalonate pathway. *Nature* **343**, 425-430. doi:10.1038/343425a0
- Gong, L., Xiao, Y., Xia, F., Wu, P., Zhao, T., Xie, S., Wang, R., Wen, Q., Zhou, W., Xu, H. et al. (2019). The mevalonate coordinates energy input and cell proliferation. *Cell Death Dis.* **10**, 327. doi:10.1038/s41419-019-1544-y
- Gonzalez, E. M., Fekany-Lee, K., Carmany-Rampey, A., Erter, C., Topczewski, J., Wright, C. V. and Solnica-Krezel, L. (2000). Head and trunk in zebrafish arise via coinhibition of BMP signaling by bozozok and chordino. *Genes Dev.* **14**, 3087-3092. doi:10.1101/gad.852400
- Grenier, J., Teillet, M.-A., Grifone, R., Kelly, R. G. and Duprez, D. (2009). Relationship between neural crest cells and cranial mesoderm during head muscle development. *PLoS ONE* **4**, e4381. doi:10.1371/journal.pone.0004381
- Grigoriadis, A. E., Heersche, J. N. M. and Aubin, J. E. (1990). Continuously growing bipotential and monopotent myogenic, adipogenic, and chondrogenic subclones isolated from the multipotential RCJ 3.1 clonal cell line. *Dev. Biol.* **142**, 313-318. doi:10.1016/0012-1606(90)90352-J
- Havis, E., Bonnin, M.-A., Olivera-Martinez, I., Nazaret, N., Ruggiu, M., Weibel, J., Durand, C., Guerin, M.-J., Bonod-Bidaud, C., Ruggiero, F. et al. (2014). Transcriptomic analysis of mouse limb tendon cells during development. *Development* **141**, 3683-3696. doi:10.1242/dev.108654
- Havis, E., Bonnin, M.-A., Esteves de Lima, J., Charvet, B., Milet, C. and Duprez, D. (2016). TGFbeta and FGF promote tendon progenitor fate and act downstream of muscle contraction to regulate tendon differentiation during chick limb development. *Development* **143**, 3839-3851. doi:10.1242/dev.136242
- Hong, L., Kenney, S. R., Phillips, G. K., Simpson, D., Schroeder, C. E., Nöth, J., Romero, E., Swanson, S., Waller, A., Strouse, J. J. et al. (2013). Characterization of a Cdc42 protein inhibitor and its use as a molecular probe. *J. Biol. Chem.* **288**, 8531-8543. doi:10.1074/jbc.M112.435941
- Huang, A. H., Watson, S. S., Wang, L., Baker, B. M., Akiyama, H., Brigande, J. V. and Schweitzer, R. (2019). Requirement for scleraxis in the recruitment of mesenchymal progenitors during embryonic tendon elongation. *Development* **146**, dev182782. doi:10.1242/dev.182782
- Hunter, M. P. and Prince, V. E. (2002). Zebrafish *hox* paralogue group 2 genes function redundantly as selector genes to pattern the second pharyngeal arch. *Dev. Biol.* **247**, 367-389. doi:10.1006/dbio.2002.0701
- Hurle, J. M., Gañan, Y. and Macias, D. (1989). Experimental analysis of the in vivo chondrogenic potential of the interdigital mesenchyme of the chick leg bud subjected to local ectodermal removal. *Dev. Biol.* **132**, 368-374. doi:10.1016/0012-1606(89)90233-9
- Hurle, J. M., Ros, M. A., Gañan, Y., Macias, D., Critchlow, M. and Hinchliffe, J. R. (1990). Experimental analysis of the role of ECM in the patterning of the distal tendons of the developing limb bud. *Cell Differ. Dev.* **30**, 97-108. doi:10.1016/0922-3371(90)90078-B
- Igel, M., Sudhop, T. and von Bergmann, K. (2001). Metabolism and drug interactions of 3-hydroxy-3-methylglutaryl coenzyme A-reductase inhibitors (statins). *Eur. J. Clin. Pharmacol.* **57**, 357-364. doi:10.1007/s002280100329
- Inman, G. J., Nicolás, F. J., Callahan, J. F., Harling, J. D., Gaster, L. M., Reith, A. D., Laping, N. J. and Hill, C. S. (2002). SB-431542 is a potent and specific inhibitor of transforming growth factor- β superfamily type I activin receptor-like kinase (ALK) receptors ALK4, ALK5, and ALK7. *Mol. Pharmacol.* **62**, 65-74. doi:10.1124/mol.62.1.65
- Istvan, E. S. and Deisenhofer, J. (2001). Structural mechanism for statin inhibition of HMG-CoA reductase. *Science* **292**, 1160-1164. doi:10.1126/science.1059344
- Jones, K. D., Couldwell, W. T., Hinton, D. R., Su, Y. H., He, S. K., Anker, L. and Law, R. E. (1994). Lovastatin induces growth inhibition and apoptosis in human malignant glioma cells. *Biochem. Biophys. Res. Commun.* **205**, 1681-1687. doi:10.1006/bbrc.1994.2861
- Jozsa, L. and Kannus, P. (1997). *Human Tendons: Anatomy, Physiology, and Pathology*. Human Kinetics: Champaign, IL.
- Kamel, G., Hoyos, T., Rochard, L., Dougherty, M., Kong, Y., Tse, W., Shubinets, V., Grimaldi, M. and Liao, E. C. (2013). Requirement for *frzb* and *fdz7a* in cranial neural crest convergence and extension mechanisms during zebrafish palate and jaw morphogenesis. *Dev. Biol.* **381**, 423-433. doi:10.1016/j.ydbio.2013.06.012
- Kardash, E., Reichman-Fried, M., Maitre, J. L., Boldajipour, B., Papisheva, E., Messerschmidt, E. M., Heisenberg, C. P. and Raz, E. (2010). A role for Rho GTPases and cell-cell adhesion in single-cell motility in vivo. *Nat. Cell Biol.* **12**, 47-53; sup pp 41-11. doi:10.1038/ncb2003
- Kieny, M. and Chevallier, A. (1979). Autonomy of tendon development in the embryonic chick wing. *J. Embryol. Exp. Morphol.* **49**, 153-165.
- Kimmel, C. B., Ballard, W. W., Kimmel, S. R., Ullmann, B. and Schilling, T. F. (1995). Stages of embryonic development of the zebrafish. *Dev. Dyn.* **203**, 253-310. doi:10.1002/aja.1002030302
- Klotz, U. (2003). Pharmacological comparison of the statins. *Arzneimittelforschung* **53**, 605-611. doi:10.1055/s-0031-1297156
- Kong, Y., Grimaldi, M., Curtin, E., Dougherty, M., Kaufman, C., White, R. M., Zon, L. I. and Liao, E. C. (2014). Neural crest development and craniofacial morphogenesis is coordinated by nitric oxide and histone acetylation. *Chem. Biol.* **21**, 488-501. doi:10.1016/j.chembiol.2014.02.013
- Kontges, G. and Lumsden, A. (1996). Rhombencephalic neural crest segmentation is preserved throughout craniofacial ontogeny. *Development* **122**, 3229-3242.
- Ladstein, R. G., Bachmann, I. M., Straume, O. and Akslen, L. A. (2010). Ki-67 expression is superior to mitotic count and novel proliferation markers PHH3, MCM4 and mitotin as a prognostic factor in thick cutaneous melanoma. *BMC Cancer* **10**, 140. doi:10.1186/1471-2407-10-140
- Laux, D. W., Febbo, J. A. and Roman, B. L. (2011). Dynamic analysis of BMP-responsive smad activity in live zebrafish embryos. *Dev. Dyn.* **240**, 682-694. doi:10.1002/dvdy.22558
- Le Douarin, N. M. and Kalcheim, C. (1999). *The Neural Crest*, 2nd edn. Cambridge University Press.
- Le Douarin, N. M. and Smith, J. (1988). Development of the peripheral nervous system from the neural crest. *Annu. Rev. Cell Biol.* **4**, 375-404. doi:10.1146/annurev.cb.04.110188.002111
- Le Lievre, C. S. (1978). Participation of neural crest-derived cells in the genesis of the skull in birds. *J. Embryol. Exp. Morphol.* **47**, 17-37.

- Léjard, V., Brideau, G., Blais, F., Salincarnboriboon, R., Wagner, G., Roehrl, M. H. A., Noda, M., Duprez, D., Houillier, P. and Rossert, J. (2007). Scleraxis and NFATc regulate the expression of the pro- α 1(I) collagen gene in tendon fibroblasts. *J. Biol. Chem.* **282**, 17665-17675. doi:10.1074/jbc.M610113200
- Lerner, E. C., Qian, Y., Hamilton, A. D. and Sebt, S. M. (1995). Disruption of oncogenic K-Ras4B processing and signaling by a potent geranylgeranyltransferase I inhibitor. *J. Biol. Chem.* **270**, 26770-26773. doi:10.1074/jbc.270.45.26770
- Lewis, K. E., Drossopoulou, G., Paton, I. R., Morrice, D. R., Robertson, K. E., Burt, D. W., Ingham, P. W. and Tickle, C. (1999). Expression of *ptc* and *gli* genes in *talpid3* suggests bifurcation in Shh pathway. *Development* **126**, 2397-2407.
- Li, F., Li, B., Wang, Q.-M. and Wang, J. H.-C. (2008). Cell shape regulates collagen type I expression in human tendon fibroblasts. *Cell Motil. Cytoskeleton* **65**, 332-341. doi:10.1002/cm.20263
- Lin, C.-Y., Yung, R.-F., Lee, H.-C., Chen, W.-T., Chen, Y.-H. and Tsai, H.-J. (2006). Myogenic regulatory factors Myf5 and Myod function distinctly during craniofacial myogenesis of zebrafish. *Dev. Biol.* **299**, 594-608. doi:10.1016/j.ydbio.2006.08.042
- Lumsden, A., Sprawson, N. and Graham, A. (1991). Segmental origin and migration of neural crest cells in the hindbrain region of the chick embryo. *Development* **113**, 1281-1291.
- Maharam, E., Yaport, M., Villanueva, N. L., Akinyibi, T., Laudier, D., He, Z., Leong, D. J. and Sun, H. B. (2015). Rho/Rock signal transduction pathway is required for MSC tenogenic differentiation. *Bone Res.* **3**, 15015. doi:10.1038/boneres.2015.15
- Mapp, O. M., Walsh, G. S., Moens, C. B., Tada, M. and Prince, V. E. (2011). Zebrafish Prickle1b mediates facial branchiomotor neuron migration via a farnesylation-dependent nuclear activity. *Development* **138**, 2121-2132. doi:10.1242/dev.060442
- Mathias, J. R., Saxena, M. T. and Mumm, J. S. (2012). Advances in zebrafish chemical screening technologies. *Future Med. Chem.* **4**, 1811-1822. doi:10.4155/fmc.12.115
- McBeath, R., Pirone, D. M., Nelson, C. M., Bhadriraju, K. and Chen, C. S. (2004). Cell shape, cytoskeletal tension, and RhoA regulate stem cell lineage commitment. *Dev. Cell* **6**, 483-495. doi:10.1016/S1534-5807(04)00075-9
- McGurk, P. D., Swartz, M. E., Chen, J. W., Galloway, J. L. and Eberhart, J. K. (2017). In vivo zebrafish morphogenesis shows Cyp26b1 promotes tendon condensation and musculoskeletal patterning in the embryonic jaw. *PLoS Genet.* **13**, e1007112. doi:10.1371/journal.pgen.1007112
- McTaggart, S. J. (2006). Isoprenylated proteins. *Cell. Mol. Life Sci.* **63**, 255-267. doi:10.1007/s00018-005-5298-6
- Miller, C. T., Yelon, D., Stainier, D. Y. R. and Kimmel, C. B. (2003). Two endothelin 1 effectors, *hand2* and *bapx1*, pattern ventral pharyngeal cartilage and the jaw joint. *Development* **130**, 1353-1365. doi:10.1242/dev.00339
- Monsoro-Burq, A.-H. and Le Douarin, N. (2000). Duality of molecular signaling involved in vertebral chondrogenesis. *Curr. Top. Dev. Biol.* **48**, 43-75. doi:10.1016/S0070-2153(08)60754-1
- Morand, O. H., Aebi, J. D., Dehmlow, H., Ji, Y. H., Gains, N., Lengsfeld, H. and Hember, J. (1997). Ro 48-8071, a new 2,3-oxidosqualene:lanosterol cyclase inhibitor lowering plasma cholesterol in hamsters, squirrel monkeys, and minipigs: comparison to simvastatin. *J. Lipid Res.* **38**, 373-390.
- Mori-Akiyama, Y., Akiyama, H., Rowitch, D. H. and de Crombrughe, B. (2003). Sox9 is required for determination of the chondrogenic cell lineage in the cranial neural crest. *Proc. Natl. Acad. Sci. USA* **100**, 9360-9365. doi:10.1073/pnas.1631288100
- Münchberg, S. R., Ober, E. A. and Steinbeisser, H. (1999). Expression of the Ets transcription factors *erm* and *pea3* in early zebrafish development. *Mech. Dev.* **88**, 233-236. doi:10.1016/S0925-4773(99)00179-3
- Murchison, N. D., Price, B. A., Conner, D. A., Keene, D. R., Olson, E. N., Tabin, C. J. and Schweitzer, R. (2007). Regulation of tendon differentiation by scleraxis distinguishes force-transmitting tendons from muscle-anchoring tendons. *Development* **134**, 2697-2708. doi:10.1242/dev.001933
- Nair, S., Li, W., Cornell, R. and Schilling, T. F. (2007). Requirements for Endothelin type-A receptors and Endothelin-1 signaling in the facial ectoderm for the patterning of skeletogenic neural crest cells in zebrafish. *Development* **134**, 335-345. doi:10.1242/dev.02704
- Nakashima, K., Zhou, X., Kunkel, G., Zhang, Z., Deng, J. M., Behringer, R. R. and de Crombrughe, B. (2002). The novel zinc finger-containing transcription factor *osterix* is required for osteoblast differentiation and bone formation. *Cell* **108**, 17-29. doi:10.1016/S0092-8674(01)00622-5
- Nichols, J. T., Blanco-Sánchez, B., Brooks, E. P., Parthasarathy, R., Dowd, J., Subramanian, A., Nachtrab, G., Poss, K. D., Schilling, T. F. and Kimmel, C. B. (2016). Ligament versus bone cell identity in the zebrafish hyoid skeleton is regulated by *mef2ca*. *Development* **143**, 4430-4440. doi:10.1242/dev.141036
- Noden, D. M. (1978). The control of avian cephalic neural crest cytodifferentiation: I. Skeletal and connective tissues. *Dev. Biol.* **67**, 296-312. doi:10.1016/0012-1606(78)90201-4
- North, T. E., Goessling, W., Walkley, C. R., Lengerke, C., Kopani, K. R., Lord, A. M., Weber, G. J., Bowman, T. V., Jang, I.-H., Grosser, T. et al. (2007). Prostaglandin E2 regulates vertebrate haematopoietic stem cell homeostasis. *Nature* **447**, 1007-1011. doi:10.1038/nature05883
- Oberlander, S. A. and Tuan, R. S. (1994). Expression and functional involvement of N-cadherin in embryonic limb chondrogenesis. *Development* **120**, 177-187.
- Ohashi, K., Osuga, J.-I., Tozawa, R., Kitamine, T., Yagyu, H., Sekiya, M., Tomita, S., Okazaki, H., Tamura, Y., Yahagi, N. et al. (2003). Early embryonic lethality caused by targeted disruption of the 3-hydroxy-3-methylglutaryl-CoA reductase gene. *J. Biol. Chem.* **278**, 42936-42941. doi:10.1074/jbc.M307228200
- Oka, K., Oka, S., Hosokawa, R., Bringas, P., Jr., Brockhoff, H. C., II, Nonaka, K. and Chai, Y. (2008). TGF- β mediated Dlx5 signaling plays a crucial role in osteochondroprogenitor cell lineage determination during mandible development. *Dev. Biol.* **321**, 303-309. doi:10.1016/j.ydbio.2008.03.046
- Pearse, R. V., II, Scherz, P. J., Campbell, J. K. and Tabin, C. J. (2007). A cellular lineage analysis of the chick limb bud. *Dev. Biol.* **310**, 388-400. doi:10.1016/j.ydbio.2007.08.002
- Piotrowski, T. and Nüsslein-Volhard, C. (2000). The endoderm plays an important role in patterning the segmented pharyngeal region in zebrafish (*Danio rerio*). *Dev. Biol.* **225**, 339-356. doi:10.1006/dbio.2000.9842
- Pryce, B. A., Watson, S. S., Murchison, N. D., Staverosky, J. A., Dunker, N. and Schweitzer, R. (2009). Recruitment and maintenance of tendon progenitors by TGF β signaling are essential for tendon formation. *Development* **136**, 1351-1361. doi:10.1242/dev.027342
- Rochard, L., Monica, S. D., Ling, I. T. C., Kong, Y., Roberson, S., Harland, R., Halpern, M. and Liao, E. C. (2016). Roles of Wnt pathway genes *wls*, *wnt9a*, *wnt5b*, *frzb* and *gpc4* in regulating convergent-extension during zebrafish palate morphogenesis. *Development* **143**, 2541-2547. doi:10.1242/dev.137000
- Ros, M. A., Rivero, F. B., Hinchliffe, J. R. and Hurle, J. M. (1995). Immunohistological and ultrastructural study of the developing tendons of the avian foot. *Anat. Embryol.* **192**, 483-496. doi:10.1007/BF00187179
- Salic, A. and Mitchison, T. J. (2008). A chemical method for fast and sensitive detection of DNA synthesis in vivo. *Proc. Natl. Acad. Sci. USA* **105**, 2415-2420. doi:10.1073/pnas.0712168105
- Santos, A. C. and Lehmann, R. (2004). Isoprenoids control germ cell migration downstream of HMGC0A reductase. *Dev. Cell* **6**, 283-293. doi:10.1016/S1534-5807(04)00023-1
- Saunders, J. W. Jr. (1948). The proximo-distal sequence of origin of the parts of the chick wing and the role of the ectoderm. *J. Exp. Zool.* **108**, 363-403. doi:10.1002/jez.1401080304
- Schilling, T. F. and Kimmel, C. B. (1994). Segment and cell type lineage restrictions during pharyngeal arch development in the zebrafish embryo. *Development* **120**, 483-494.
- Schweitzer, R., Chyung, J. H., Murtaugh, L. C., Brent, A. E., Rosen, V., Olson, E. N., Lassar, A. and Tabin, C. J. (2001). Analysis of the tendon cell fate using Scleraxis, a specific marker for tendons and ligaments. *Development* **128**, 3855-3866.
- Shimizu, N., Kawakami, K. and Ishitani, T. (2012). Visualization and exploration of Tcf/Lef function using a highly responsive Wnt/ β -catenin signaling-reporter transgenic zebrafish. *Dev. Biol.* **370**, 71-85. doi:10.1016/j.ydbio.2012.07.016
- Shutes, A., Onesto, C., Picard, V., Leblond, B., Schweighoffer, F. and Der, C. J. (2007). Specificity and mechanism of action of EHT 1864, a novel small molecule inhibitor of Rac family small GTPases. *J. Biol. Chem.* **282**, 35666-35678. doi:10.1074/jbc.M703571200
- Signore, I. A., Jerez, C., Figueroa, D., Suazo, J., Marcelain, K., Cerda, O. and Colombo Flores, A. (2016). Inhibition of the 3-hydroxy-3-methyl-glutaryl-CoA reductase induces orofacial defects in zebrafish. *Birth Defects Res. A Clin. Mol. Teratol.* **106**, 814-830. doi:10.1002/bdra.23546
- Soeda, T., Deng, J. M., de Crombrughe, B., Behringer, R. R., Nakamura, T. and Akiyama, H. (2010). Sox9-expressing precursors are the cellular origin of the cruciate ligament of the knee joint and the limb tendons. *Genesis* **48**, 635-644. doi:10.1002/dvg.20667
- Soldatov, R., Kaucka, M., Kastrić, M. E., Petersen, J., Chontorotzea, T., Englmaier, L., Akkuratova, N., Yang, Y., Häring, M., Dyachuk, V. et al. (2019). Spatiotemporal structure of cell fate decisions in murine neural crest. *Science* **364**, eaas9536. doi:10.1126/science.aas9536
- Solursh, M., Linsenmayer, T. F. and Jensen, K. L. (1982). Chondrogenesis from single limb mesenchyme cells. *Dev. Biol.* **94**, 259-264. doi:10.1016/0012-1606(82)90090-2
- Spadari, S., Pedrali-Noy, G., Ciomei, M., Falaschi, A. and Ciarrocchi, G. (1984). Control of DNA replication and cell proliferation in eukaryotes by aphidicolin. *Toxicol. Pathol.* **12**, 143-148. doi:10.1177/019262338401200205
- Stringa, E. and Tuan, R. S. (1996). Chondrogenic cell subpopulation of chick embryonic calvarium: isolation by peanut agglutinin affinity chromatography and in vitro characterization. *Anat. Embryol.* **194**, 427-437. doi:10.1007/BF00185990
- Subramanian, A. and Schilling, T. F. (2014). Thrombospondin-4 controls matrix assembly during development and repair of myotendinous junctions. *eLife* **3**, e02372. doi:10.7554/eLife.02372
- Sugimoto, Y., Takimoto, A., Akiyama, H., Kist, R., Scherer, G., Nakamura, T., Hiraki, Y. and Shukunami, C. (2013). Sox+/Sox9+ progenitors contribute to the establishment of the junction between cartilage and tendon/ligament. *Development* **140**, 2280-2288. doi:10.1242/dev.096354
- Suster, M. L., Abe, G., Schouw, A. and Kawakami, K. (2011). Transposon-mediated BAC transgenesis in zebrafish. *Nat. Protoc.* **6**, 1998-2021. doi:10.1038/nprot.2011.416

- Tan, G.-K., Pryce, B. A., Stabio, A., Brigande, J. V., Wang, C. J., Xia, Z., Tufa, S. F., Keene, D. R. and Schweitzer, R.** (2020). Tgfb signaling is critical for maintenance of the tendon cell fate. *eLife* **9**, e52695. doi:10.7554/eLife.52695
- ten Berge, D., Brugmann, S. A., Helms, J. A. and Nusse, R.** (2008). Wnt and FGF signals interact to coordinate growth with cell fate specification during limb development. *Development* **135**, 3247-3257. doi:10.1242/dev.023176
- Thisse, B., Pflumio, S., Fürthauer, M., Loppin, B., Heyer, V., Degraeve, A., Woehl, R., Lux, A., Steffan, T., Charbonnier, X. Q. et al.** (2001). Expression of the zebrafish genome during embryogenesis (NIH R01 RR15402). ZFIN Direct Data Submission. <https://zfin.org/ZDB-PUB-010810-1>
- Thorpe, J. L., Doitsidou, M., Ho, S.-Y., Raz, E. and Farber, S. A.** (2004). Germ cell migration in zebrafish is dependent on HMGC0A reductase activity and prenylation. *Dev. Cell* **6**, 295-302. doi:10.1016/S1534-5807(04)00032-2
- Trainor, P. A. and Krumlauf, R.** (2000). Patterning the cranial neural crest: hindbrain segmentation and Hox gene plasticity. *Nat. Rev. Neurosci.* **1**, 116-124. doi:10.1038/35039056
- Uehata, M., Ishizaki, T., Satoh, H., Ono, T., Kawahara, T., Morishita, T., Tamakawa, H., Yamagami, K., Inui, J., Maekawa, M. et al.** (1997). Calcium sensitization of smooth muscle mediated by a Rho-associated protein kinase in hypertension. *Nature* **389**, 990-994. doi:10.1038/40187
- von der Mark, K., Gauss, V., von der Mark, H. and Müller, P.** (1977). Relationship between cell shape and type of collagen synthesised as chondrocytes lose their cartilage phenotype in culture. *Nature* **267**, 531-532. doi:10.1038/267531a0
- Westerfield, M.** (2000). *The Zebrafish Book. A Guide for the Laboratory use of Zebrafish (Danio rerio)*, 4th edn. Eugene, OR: University of Oregon Press.
- Woods, A., Wang, G., Dupuis, H., Shao, Z. and Beier, F.** (2007). Rac1 signaling stimulates N-cadherin expression, mesenchymal condensation, and chondrogenesis. *J. Biol. Chem.* **282**, 23500-23508. doi:10.1074/jbc.M700680200
- Wortham, R. A.** (1948). The development of the muscles and tendons in the lower leg and foot of chick embryos. *J. Morphol.* **83**, 105-148. doi:10.1002/jmor.1050830106
- Xu, H., Kardash, E., Chen, S., Raz, E. and Lin, F.** (2012). Gbetagamma signaling controls the polarization of zebrafish primordial germ cells by regulating Rac activity. *Development* **139**, 57-62. doi:10.1242/dev.073924
- Yamamoto-Shiraishi, Y.-I. and Kuroiwa, A.** (2013). Wnt and BMP signaling cooperate with Hox in the control of Six2 expression in limb tendon precursor. *Dev. Biol.* **377**, 363-374. doi:10.1016/j.ydbio.2013.02.023
- Yan, Y.-L., Hatta, K., Riggleman, B. and Postlethwait, J. H.** (1995). Expression of a type II collagen gene in the zebrafish embryonic axis. *Dev. Dyn.* **203**, 363-376. doi:10.1002/aja.1002030308
- Yan, Y. L., Miller, C. T., Nissen, R. M., Singer, A., Liu, D., Kirn, A., Draper, B., Willoughby, J., Morcos, P. A., Amsterdam, A. et al.** (2002). A zebrafish sox9 gene required for cartilage morphogenesis. *Development* **129**, 5065-5079.
- Yan, Y.-L., Willoughby, J., Liu, D., Crump, J. G., Wilson, C., Miller, C. T., Singer, A., Kimmel, C., Westerfield, M. and Postlethwait, J. H.** (2005). A pair of Sox: distinct and overlapping functions of zebrafish sox9 co-orthologs in craniofacial and pectoral fin development. *Development* **132**, 1069-1083. doi:10.1242/dev.01674
- Yi, P., Han, Z., Li, X. and Olson, E. N.** (2006). The mevalonate pathway controls heart formation in *Drosophila* by isoprenylation of Ggamma1. *Science* **313**, 1301-1303. doi:10.1126/science.1127704

Supplemental Figures

Fig. S1. Expression pattern of *scxa* and *Tg(scxa:mcherry)*. (A-C') *scxa* expression at 32hpf, 48hpf, and 72hpf in wild-type embryos. (D-F') *mcherry* expression at 32hpf, 48hpf, and 72hpf in *Tg(scxa:mcherry)* embryos. Black arrow, *scxa* or *mcherry* expression in the pharyngeal arches. Lateral (A-F) and ventral (A'-F') view, anterior to the left.

FIGURE S1.

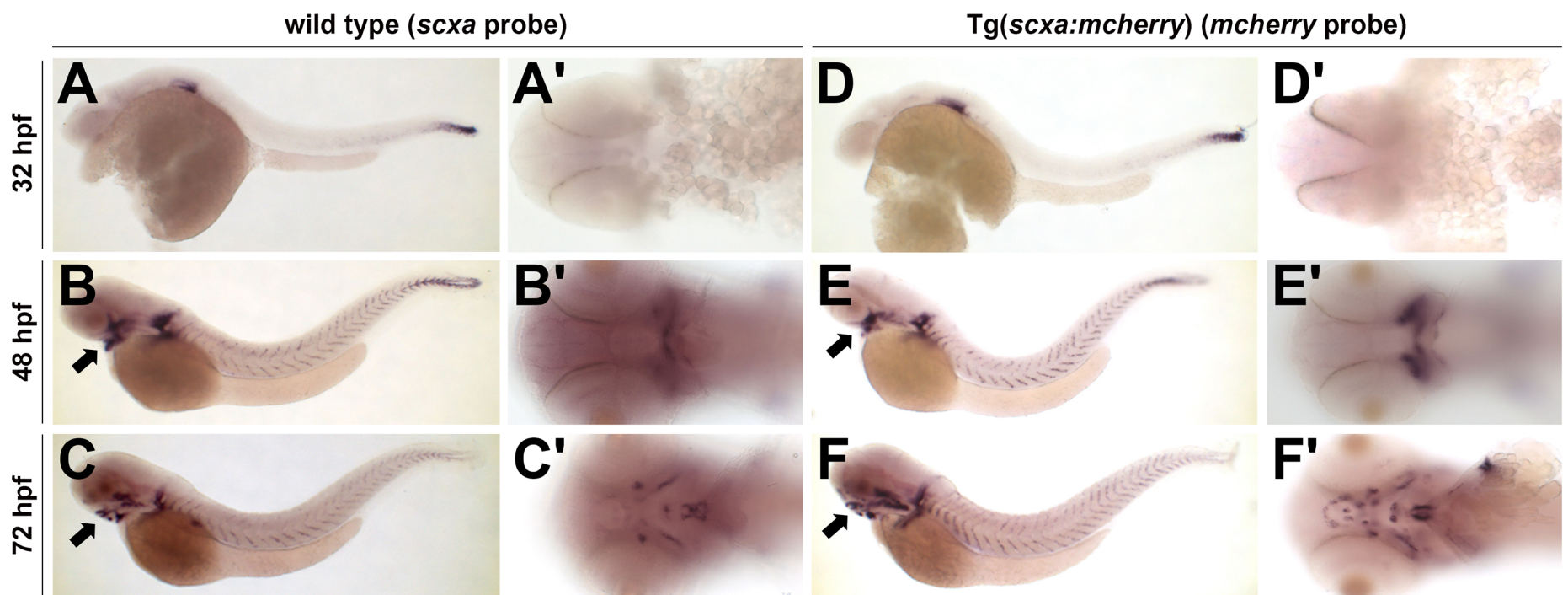


Fig. S2. Effect of statin treatment on zebrafish tendon development. (A-F) *scxa* expression at 56hpf upon chemical incubation from 32-56hpf. *scxa* is expressed in the ventral jaw region (arrow) of DMSO-treated embryos (A) and expression lost in SU5402-treated embryos (B), controls in the chemical screen. Lovastatin (C) and simvastatin (D), positive hits identified from the screen, caused expansion of *scxa* in the ventral craniofacial region (arrow) compared with controls. Commercially available statins that differ in their pharmacokinetics, atorvastatin (E) and fluvastatin (F), caused similar expansion of *scxa* in the ventral craniofacial region (arrow) compared with controls. (G-L) *scxa* expression at 56hpf upon chemical incubation from 32-56 hpf. Atorvastatin (I-L) caused a dose-dependent expansion of *scxa* in the ventral craniofacial region (arrow) compared with controls (G, H). (M-P) *scxa* expression at 48hpf and 56hpf upon chemical incubation from 32-48 hpf. Fluvastatin caused an expansion of *scxa* in the ventral craniofacial region (arrow) at 56hpf compared with control. (Q, R) *scxa* expression is not expanded at 56 hpf upon chemical incubation from 48-56 hpf. (S-U) *runx2a* expression at 56hpf and 72hpf upon chemical incubation from 32-56 hpf and 48-72 hpf, respectively. Atorvastatin affected the morphology of the *runx2a* expression domain at 56 hpf. At 72 hpf, treatment caused a significant reduction of *runx2a* expression in the ventral craniofacial region compared with control. (W, X) Pectoral fin *colla2* expression at 74hpf upon chemical incubation from 32-56 hpf. (Y) Quantification of myoseptal *scxa:mcherry*⁺ cells at 56 hpf and 72 hpf upon chemical incubation from 32-56 hpf and 48-72 hpf, respectively. Atorvastatin does not increase the quantity of myoseptal *scxa:mcherry*⁺ cells at 56hpf or 72hpf compared with controls. (Z-C') Myoseptal expression of Tg(*scxa:mcherry*) at 56hpf and 72hpf upon chemical incubation from 32-56hpf and 48-72hpf, respectively. (D', E') Myoseptal expression of *colla2* at 74hpf upon chemical incubation from 32-56hpf. Atorvastatin caused a reduction in myoseptal expression of *colla2* compared with controls. For cell counts (Y), red bars indicate mean; points represent individual embryos; Mann-Whitney-Wilcoxon test. N.S, no significance. Ventral (A-F, H, J, L, M-V) and lateral (G, I, K, W, X, Z-E') views of flat-mounted embryos, anterior to the left.

FIGURE S2.

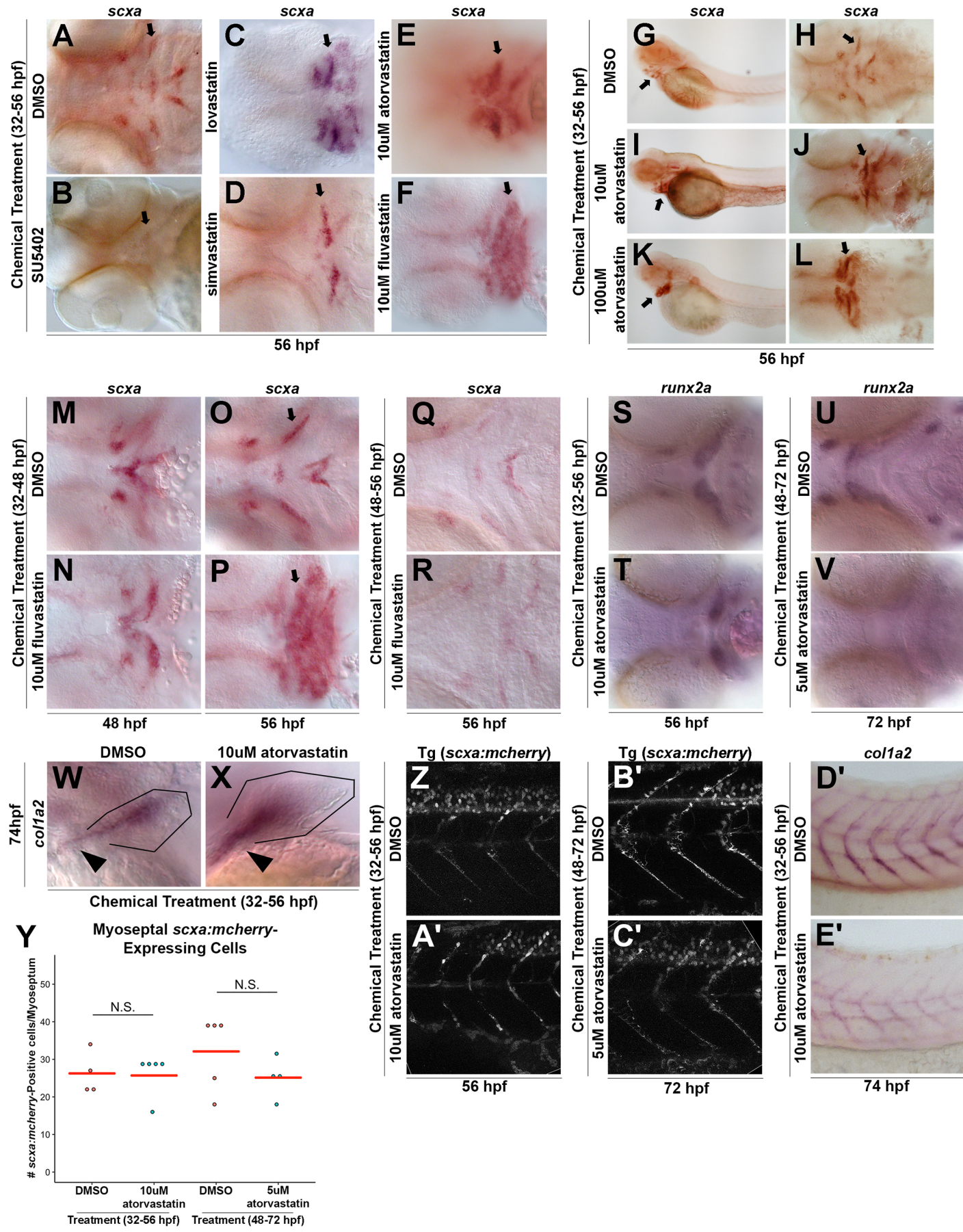


Fig. S3. Analysis of proliferation in statin-treated pectoral fin and craniofacial *scxa*-positive tendon progenitors. (A) Quantification of craniofacial cells expressing PH3 at 56hpf upon chemical incubation from 32-56hpf. (B-D) Quantification of pectoral fin cells expressing *scxa*, PH3, and co-expressing PH3 and *scxa* at 56hpf upon chemical incubation from 32-56hpf, as assessed from confocal images of embryos processed by fluorescent *in situ* hybridization and immunohistochemistry, and counterstained with Hoechst33342. (E-H) Craniofacial expression of *scxa* at 56hpf upon chemical incubation from 32-56hpf. *scxa* expression, compared with controls (E, arrow), is reduced in embryos treated with Aphidicolin (F, arrow), and expanded in embryos treated with atorvastatin alone (G, arrow) and in combination with Aphidicolin (H, arrow). (I) Experimental design for counting *scxa*- and *colla2*-expressing cells (Fig. 1L, 1N, 2I, 5O, S3B), *scxa:mcherry*-expressing cells (Fig. 1M, S2Y), PH3-positive cells (Fig. S3A, S3C), and PH3 and *scxa* co-expressing cells (Fig. 2H, S3D). (J-K) Example of quantification of *scxa:mcherry*-expressing cells in the pectoral fin at 56hpf upon chemical incubation from 32-56hpf, corresponding to (Fig. 1F-G). (L-Q) Examples of quantification of *scxa*- and PH3-expressing cells in the craniofacial region at 56hpf upon chemical incubation from 32-56hpf, corresponding to (Fig. 2D-H). For cell counts (A-D), red bars indicate mean; points represent individual embryos; Mann-Whitney-Wilcoxon test. N.S., no significance; ***, P<0.001; ****, P<0.0001. MIP, maximum intensity projection.

FIGURE S3.

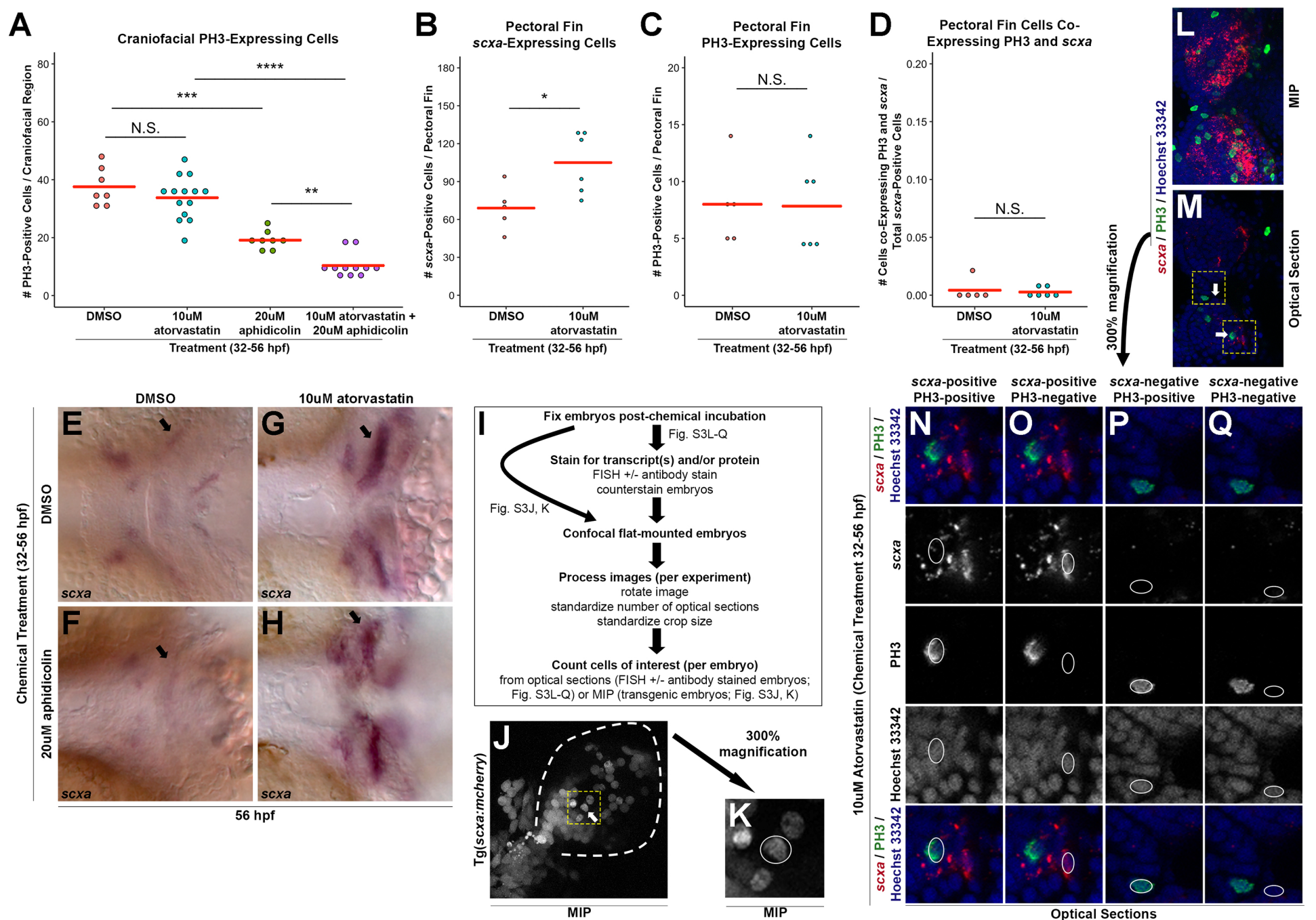


Fig. S4. Effect of statin on pectoral fin musculoskeleton and CNC origin of expanded craniofacial *scxa* cells. (A-H) Expression of *sox9a*, *col2a1*, *sox10:eGFP*, and *myod1* at 56hpf in the pectoral fin upon chemical incubation from 32-56hpf. At 56hpf, atorvastatin caused a s alteration in the expression of *sox9a* (A, B), *col2a1* (C, D), *sox10:eGFP* (E, F), and *myod1* (H). (I-L) Expression of Kaede and *scxa* in Tg(*sox10:kaede*) embryos at 56hpf upon chemi incubation from 32-56hpf. Co-localization of Kaede and *scxa* at 56hpf is observed in virtua *scxa*⁺ domains of DMSO- and atorvastatin-treated embryos (white arrow). Yellow-colored boxe mark the craniofacial domain in the maximum-intensity projection (I, K) that is magnified i corresponding optical section (J, L). Ventral (I-L) and lateral (A-H) views of flat-mounted embryos, anterior to the left. MIP, maximum intensity projection.

FIGURE S4.

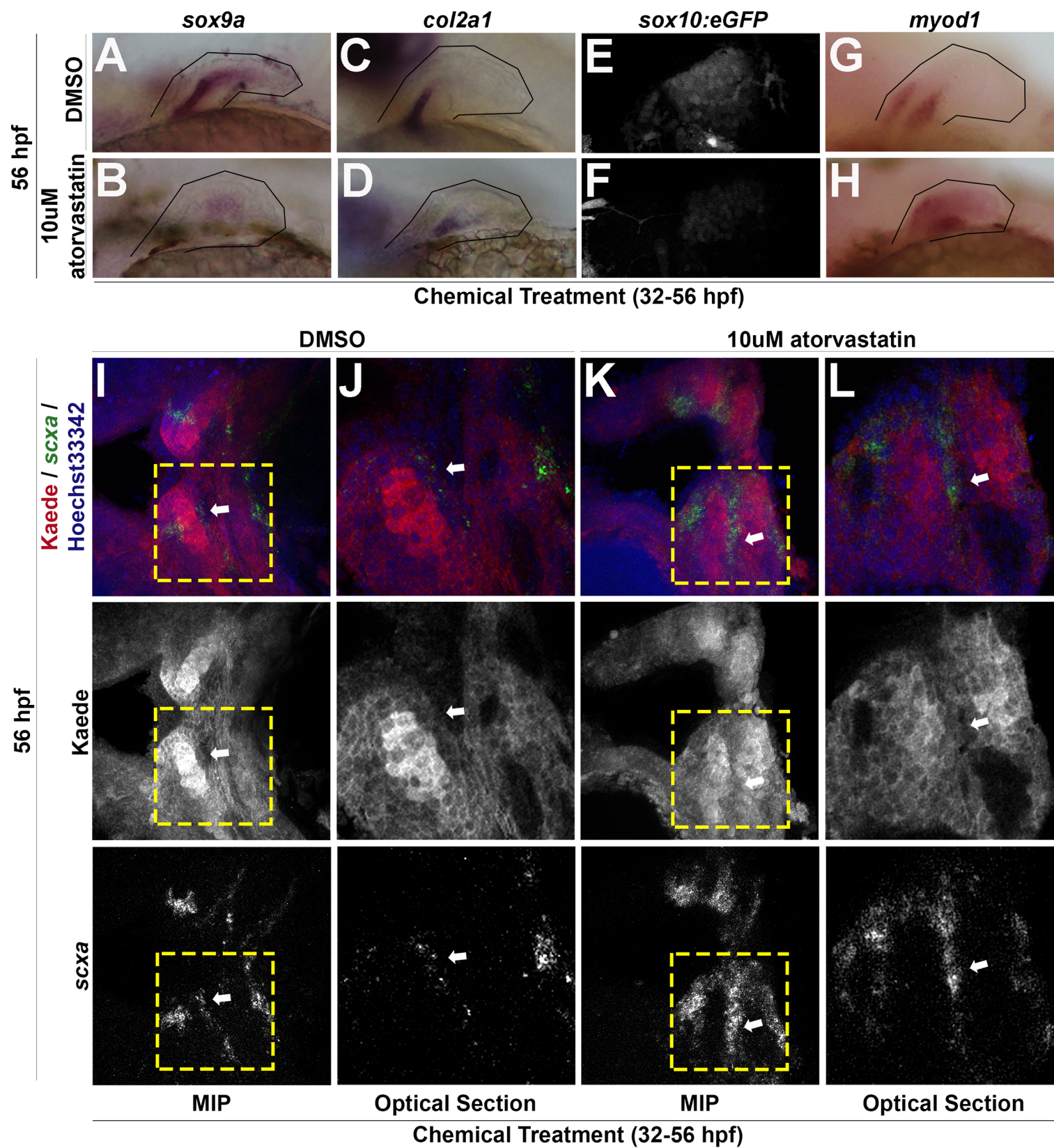


Fig. S5. Effect of statin on pharyngeal arch patterning. Craniofacial expression of markers of craniofacial patterning and associated with characterized signaling pathways. **(A-P)** Expression at 48hpf upon chemical incubation from 32-48hpf. **(A, B)** Atorvastatin caused expansion of *scxa* expression compared with controls. Atorvastatin did not drastically alter expression of **(C-F)** anterior-posterior (*hoxa2b*, *hoxb2a*) or **(G-J)** dorsal-ventral (*hand2*, *bapx1*) arch polarity markers compared with controls. Atorvastatin did not cause expansion in expression of markers associated with **(K-M)** Hedgehog (*shha*, *patched1*) and **(N)** Bmp (*bmp4*) signaling, compared with controls. **(O-R)** Craniofacial expression upon chemical incubation starting at 32hpf. Atorvastatin did not cause expansion in expression of markers associated with TGFβ (*tgfbr2a*, *tgfbi*) signaling at **(O, P)** 48hpf or **(Q)** 56hpf compared with controls. **(R)** Atorvastatin caused a reduction in *gsc* expression compared with controls at 56hpf, likely due to developmental delay, but its spatial expression in arch 1-2 was appropriate. **(S-X)** Craniofacial expression at 48hpf upon chemical incubation from 32-48hpf. Atorvastatin did not cause expansion in expression of markers associated with **(S, T)** FGF (*pea3*) or **(U-X)** Wnt (*fzd7a*, *fzd7b*) signaling compared with controls. **(Y-B')** Expression of Tg(*6xTcf/LefBS-miniP:d2eGFP*) at 56hpf and 72hpf upon chemical incubation from 32-56hpf and 48-72hpf, respectively. Atorvastatin did not cause expansion of the *d2eGFP* reporter of Wnt/β-catenin-mediated Tcf transcriptional activity at 56hpf or 72hpf compared with controls. Ventral (**B, D, F, H, J, L, Q, R, T, V, X-Z, A', B'**) and lateral (**A, C, E, G, I, K, M-P, S, U, W**) views of flat-mounted embryos, anterior to the left.

FIGURE S5.

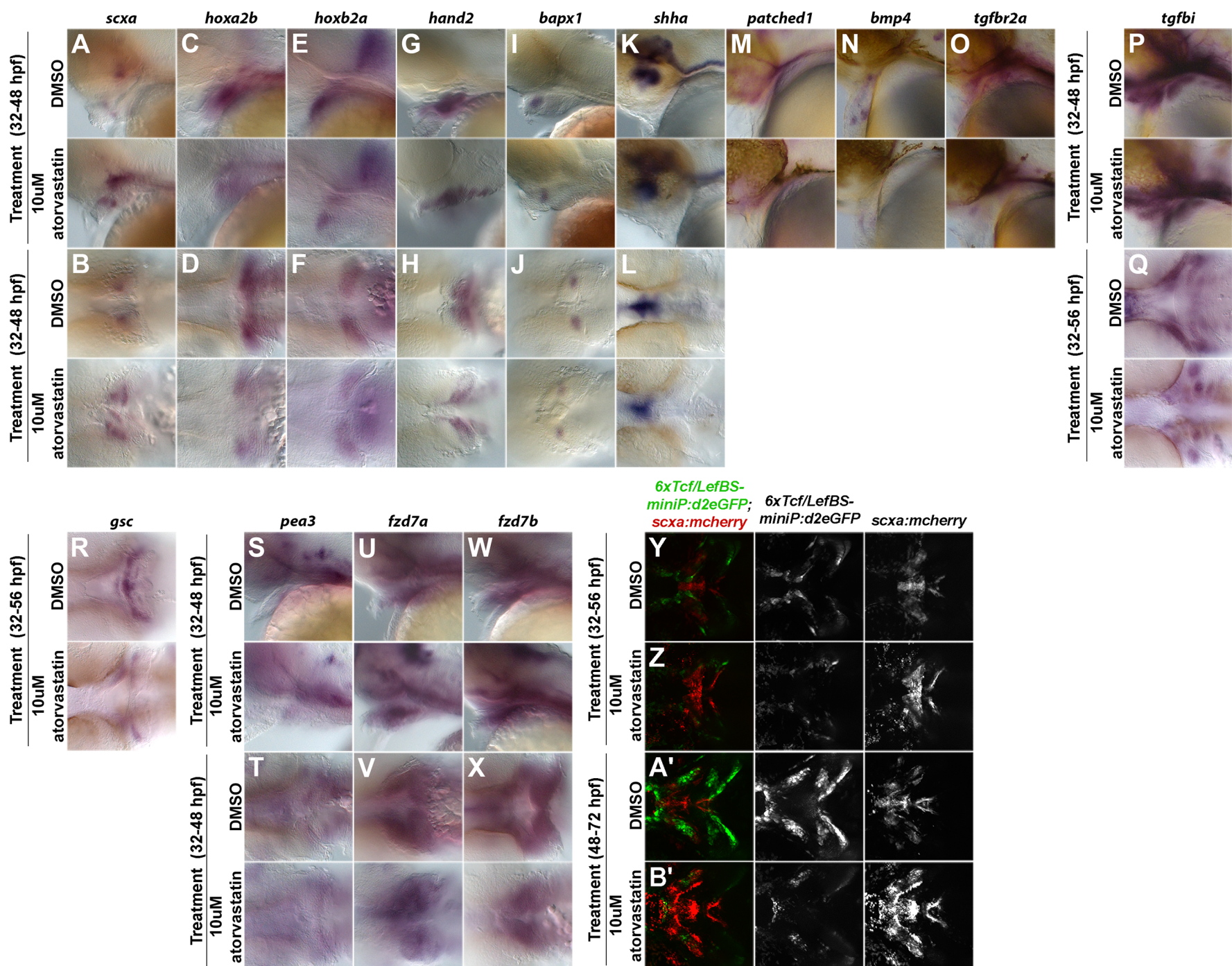


Fig. S6. Analysis of BMP and TGF β signaling in the craniofacial region of statin treated embryos. (A-F) *egfp* expression in Tg(*bre:egfp*) embryos at 56hpf upon chemical incubation from 32-56hpf. Atorvastatin did not expand expression of the BMP reporter line Tg(*bre:egfp*) but altered spatial expression of *egfp* around the mouth and posterior pharyngeal arch region, compared to controls. White asterisk, presumptive mouth opening; white arrow, maxillary process; red arrow, mandibular process; yellow arrow, posterior pharyngeal arch region. (G) Inhibition of TGF β signaling (SB431542) reduced *scxa* and increased *sox9a* at 56hpf upon 32-56hpf incubation, compared with DMSO controls. The combination of statin treatment and inhibition of TGF β signaling amplified the increase in *sox9a* expression and rescued *scxa* expression to levels comparable to that of the DMSO controls. N=3, head region, Welch's 2-tailed t-test. (H-S') Expression of Phospho-Smad3 in Tg(*col2a1a:eGFP*; *scxa:mcherry*) embryos at 56hpf upon chemical incubation from 32-56hpf. Atorvastatin altered the pattern of Phospho-Smad3 staining compared to controls (compare cyan arrow in **K'** and **Q'**), but was not co-expressed with *scxa:mcherry*. White arrow, Phospho-Smad3 staining in a lateral region near the palatoquadrate cartilage; cyan arrow, Phospho-Smad3 staining in a medial region near Meckel's cartilage; red arrow, *scxa:mcherry*⁺ tendon cell; green arrow, *col2a1a:eGFP*⁺ palatoquadrate cartilage. MIP, Maximum Intensity Projection. Ventral (A-F, H-S') views of live (A-F) and fixed (H-S') embryos, anterior to the left. N.S, no significance; *, P<0.05; **, P<0.01; ***, P<0.001.

FIGURE S6.

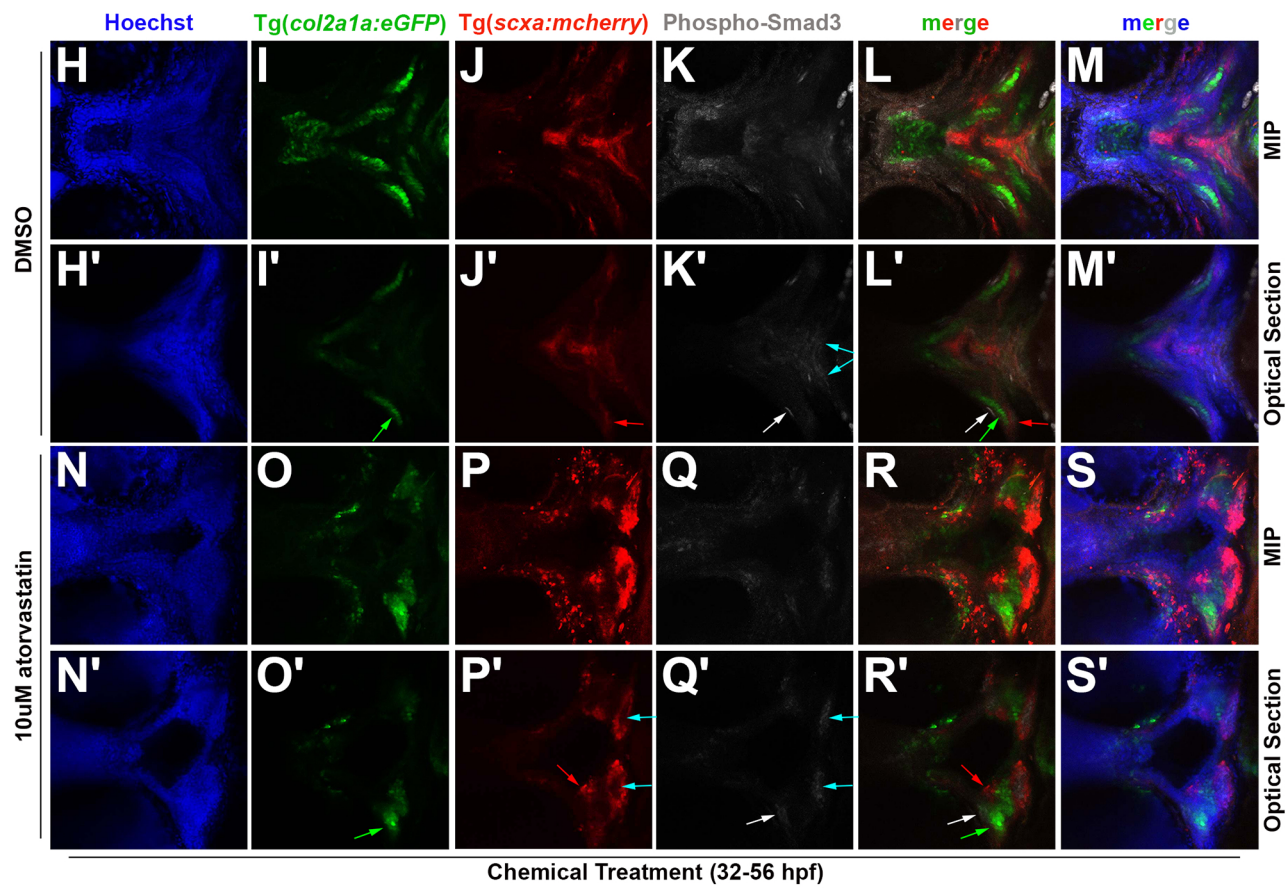
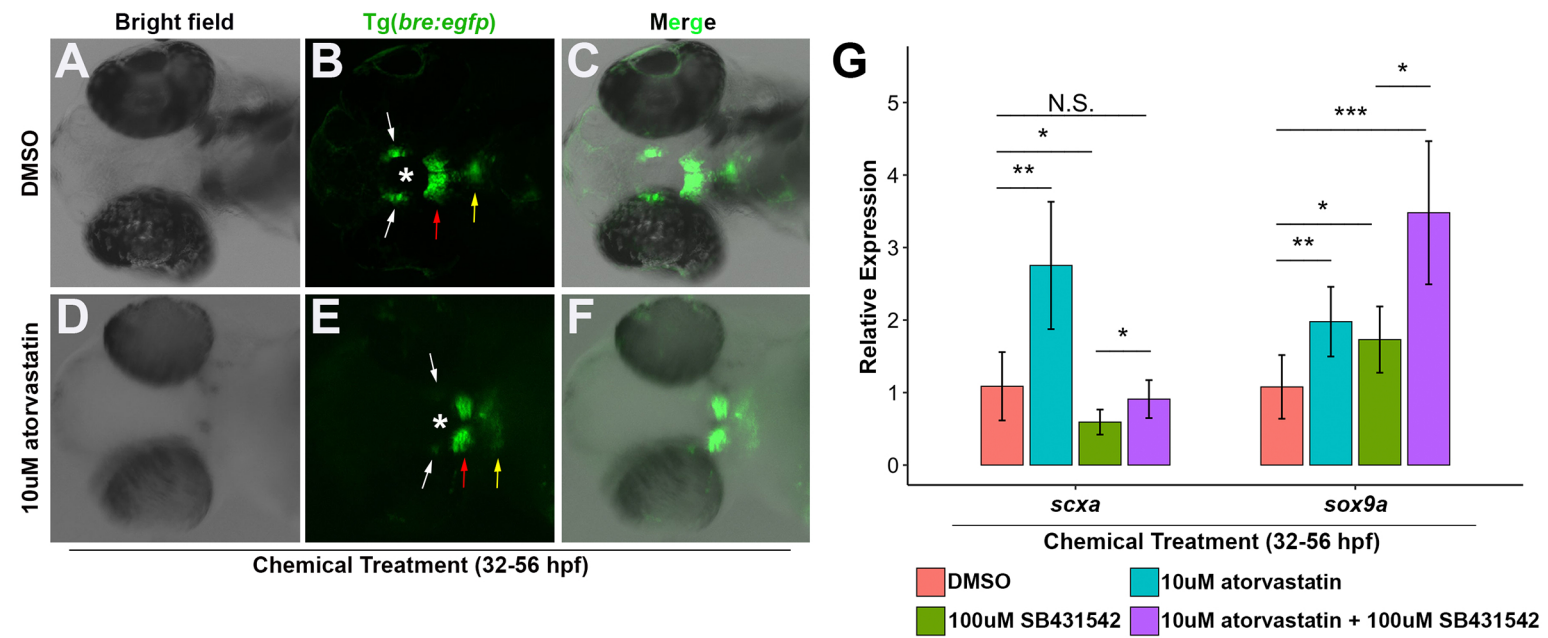


Fig. S7. Role of the mevalonate pathway in statin-mediated expansion of *scxa*-positive tendon progenitors. (A-D) Craniofacial expression of *scxa* at 60hpf (A, B, 100% mutants expanded expression, n=36) and *col1a2* at 76hpf (C, D, 83% mutants expanded, n=23) is expanded in the *hmgcr1b*_{s617} mutants, identified by their severe pericardial edema. (E-H) Craniofacial expression of *scxa* is expanded at 56hpf in embryos exposed to synergistic interaction of *hmgcr1b* morpholino-mediated knockdown and chemical treatment from 32-56hpf (H), but not in singly chemically treated (F) or in MO-injected embryos (G). (I-K) Craniofacial expression of *scxa* at 56hpf, compared with controls (I, 100%, n=6), is expanded upon co-treatment with GGTI-286, RO48-8071, and FTI-277 following chemical incubation from 32-56hpf (J, 30%; n=10). This expansion in *scxa* expression phenocopies that of atorvastatin-treated embryos (K). Arrows indicate craniofacial domain where *scxa* is expanded in statin-treated embryos. Ventral views of flat-mounted embryos, anterior to the left.

FIGURE S7.

